energies

MDPI

Review

The Impact of Additives on the Main Properties of Phase Change Materials

Ewelina Radomska *, Lukasz Mika and Karol Sztekler

Department of Thermal and Fluid Flow Machines, Faculty of Energy and Fuels, AGH University of Science and Technology, Mickiewicza 30 St., 30-059 Krakow, Poland; lmika@agh.edu.pl (L.M.); sztekler@agh.edu.pl (K.S.)

* Correspondence: radomska@agh.edu.pl

Received: 11 May 2020; Accepted: 11 June 2020; Published: 13 June 2020

Abstract: The main drawback of phase change materials (PCMs) is their low thermal conductivity, which limits the possibilities of a wide range of implementations. Therefore, the researchers, as found in the literature, proposed several methods to improve the thermal conductivity of PCMs, including inserting high thermal conductivity materials in nano-, micro-, and macro-scales, as well as encapsulation of PCMs. However, these inserts impact the other properties of PCMs like latent heat, melting temperature, thermal stability, and cycling stability. Hence, this paper aims to review the available in the open literature research on the main properties of enhanced PCMs that undergo solid–liquid transition. It is found that inserting high thermal conductivity materials and encapsulation results in improved thermal conductivity of PCMs, but it decreases their latent heat. Moreover, the insertions can act as nucleating agents, and the supercooling degree can be reduced. Some of the thermal conductivity enhancers (TCEs) may prevent PCMs from leakage. However, some test results are inconsistent and some seem to be questionable. Therefore, this review indicates these discrepancies and gaps in knowledge and points out possible directions for further research.

Keywords: phase change materials; latent heat; melting time; thermal conductivity; thermal stability; cycling stability; solid–liquid transition

1. Introduction

Globally, in 2017, the total primary energy supply (TPES) was 13,972 Mtoe, of which about 81% was from fossil fuels like coal, oil, and natural gas [1]. Burning fossil fuels results in the release of harmful substances like greenhouse gases, including CO_2, which contribute to climate change. Moreover, fossil fuel resources are limited, and they must also be converted to a usable form of energy, which is usually related to heat generation. On the other hand, according to the International Energy Agency [1], the share of renewable energy sources (RES) in the TPES is growing. The main disadvantage of RES is their unpredictability, resulting in a mismatch between demand and supply. Due to the abovementioned reasons, fossil fuels should be saved through increasing the efficiency of processes in the energy supply chain, and reduction the abovementioned mismatch. One of the solutions, or at least the minimization of these problems, is to implement thermal energy storage (TES).

There are three main types of TES, depending on the occurred phenomenon: sensible, latent, and thermochemical [2]. In sensible thermal energy storage (STES), heat is stored by increasing the temperature of a material. In STES, solid materials like rocks, metals, concrete, sand, bricks, and liquid materials like water or ethanol are usually used [3]. Latent heat thermal energy storage (LHTES) comes from isothermal or near isothermal heat absorption and release during the phase change of a material [4]. Materials that store latent heat are called phase change materials (PCMs). The third type

of TES is called thermochemical heat storage [2], chemical heat storage [5], or sometimes sorption heat storage [6]. In this type of TES, heat is absorbed/released during reversible endothermic/exothermic chemical reactions or sorption processes [3,5]. Each of the abovementioned techniques provides different possibilities of heat storage, and their properties, advantages, disadvantages, and comparison can be found elsewhere in the literature [2,7–9]. PCMs are promising heat storage materials due to their ability to store 5–14 times more heat per unit volume than sensible heat storage materials, and their main advantage is that they absorb and release heat at a nearly constant temperature [10]. PCMs can be classified according to two criteria: chemical composition and type of phase transition [11]. The classification of PCMs depending on chemical composition and type of phase transition based on [10–12] is presented in Figure 1.

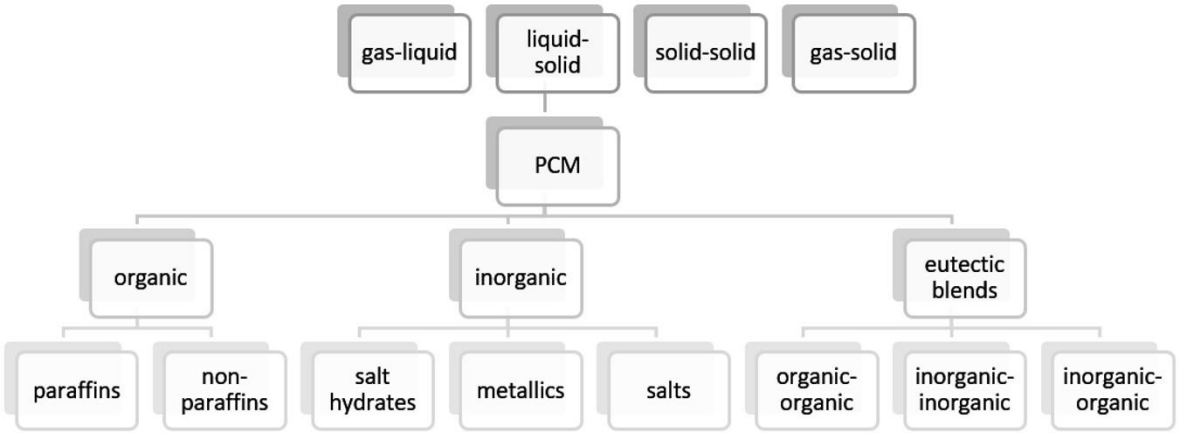

Figure 1. Classification of phase change materials (PCMs) depending on phase transition (top) and chemical composition (bottom) [10–12].

Solid–liquid transition is the most commonly used type because of its large heat storage density and relatively small volume changes compared to solid–gas or liquid–gas transitions in which occurring gas occupies a large volume [13]. Solid–solid PCMs had not gained much attention yet mainly due to their low phase transition enthalpies [13], so this paper focuses only on solid–liquid PCMs and in the following parts of paper the term PCM will stand for only solid–liquid PCMs. The second classification of PCMs, based on chemical composition, divided them mainly into organic and inorganic due to their different chemical structure and various properties, which can be found elsewhere in the literature [10,12]. Required properties of PCMs include for example high latent and specific heat, high thermal conductivity, high density, small volume changes, suitable phase change temperature, low supercooling, good thermal stability, and good cycling stability [10–12,14]. Good cycling stability means no change in the PCM properties after many melting and solidification cycles. Detailed data on PCMs properties can be found elsewhere in the literature [7,8,10,12,15].

Due to the possibility of holding a large amount of heat, phase change materials may be used in many different applications such as maintaining thermal comfort in buildings by incorporating PCMs into floors, walls or ceilings [16], thermal energy storage of waste heat [17], thermal energy storage in domestic hot water systems [18], solar applications [19–21], thermal management of batteries [22], and electronic devices [23], incorporating PCMs into textiles to maintain constant body temperature [24], increasing cooling performance of air-conditioning units [25], the food industry [26], medicine [27] and many others which can be found in [28–31]. Although PCMs have many advantages over other TES technologies, their main drawback is low thermal conductivity, which in the solid state varies from approximately 0.6 W/(m·K) to 1.3 W/(m·K) for inorganic PCMs, and from approximately 0.2 W/(m·K) to 0.7 W/(m·K) for organic PCMs [8,12]. The low thermal conductivity of PCMs limits in practice the possibilities of a wide range of implementations. However, it is worth mentioning that there is a group of promising PCMs, i.e., metal alloys, with relatively high thermal conductivities [32], but due to their high thermal conductivity, they are not discussed in this paper. Melting

temperatures, latent heat of fusion, and thermal conductivities of selected PCMs are presented in Table 1.

Table 1. Properties of selected PCMs [8,12].

PCM	Melting Temperature, (°C)	Latent Heat, (kJ/kg)	Thermal Conductivity, (W/(m·K))	
			Liquid State	Solid State
Organic				
n-Tetradecane (C14)	6	229	not available	0.21
n-Octadecane (C18)	28.4	244	0.148	0.358
Caprylic acid	16	148.6	0.149	not available
Naphthalene	80	147.7	0.132	0.341
Erythritol	118.0	339.8	0.326	0.733
Inorganic				
$CaCl_2$ 6 H_2O	29	190.8	0.540	1.088
$Ba(OH)_2$ 8 H_2O	78	265.7	0.653	1.255
$Mg(NO_3)_2$ 6 H_2O	89	162.8	0.490	0.611
$MgCl_2$ 6 H_2O	117	168.6	0.570	0.694
KNO_3	333	266.0	0.5 [1]	

[1] No data regarding the physical state of the material.

Due to the low thermal conductivity of PCMs, several methods of heat transfer enhancement in LHTES were proposed. The equation of heat transfer rate in the simplest form can be written as:

$$\dot{Q} = U\ A\ \Delta T, \quad (1)$$

where $\dot{Q}$, U, A, and ΔT are the heat transfer rate (W), overall heat transfer coefficient (W/(m^2·K)), surface area (m^2), and temperature difference (°C), respectively. According to Equation (1), the heat transfer rate can be improved by increasing the overall heat transfer coefficient, surface area, or temperature difference. Overall heat transfer coefficient depends, among others, on the thermal conductivity of a material. Thus, heat transfer enhancement techniques in LHTES can be divided into four main groups:

1. improving thermal properties, especially the thermal conductivity of a material,
2. increasing the heat transfer surface area,
3. improving the heat transfer process,
4. combined (hybrid) techniques.

Increasing the thermal conductivity of PCMs can be achieved by inserting high thermal conductivity materials into PCMs. Increasing the heat transfer surface area can be achieved by using fins or encapsulation PCMs. The third method includes using heat pipes, multiple PCMs, modifications of heat exchanger constructions, or changing process conditions, for example, by increasing heat transfer fluid (HTF) temperature and/or flow rate. Heat pipes can improve the heat transfer between HTF and PCM due to the evaporation and condensation of a working fluid, which results in a high heat transfer coefficient, thus augmenting the heat transfer between the HTF and PCM. Like was mentioned, the heat transfer rate between the HTF and PCM depends, among others, on the temperature difference between them. However, as the HTF flows through the heat exchanger, its temperature decreases, thus the temperature difference between the HTF and PCM also decreases. Therefore, to overcome the problem of decreasing temperature difference, multiple PCMs, i.e., PCMs with decreasing melting temperatures located along the HTF flow path, which ensures the constant temperature difference between the PCM and HTF. Constructions of heat exchangers can be modified in different ways, for example, Kadivar et al. [33] designed the double-tube heat exchanger with a non-concentric inner tube, which enhanced the natural convection and reduced the melting time of PCM. Combined techniques consist of a combination of at least two different techniques listed above.

The proposed classification of heat transfer enhancement techniques in LHTES is presented in Figure 2.

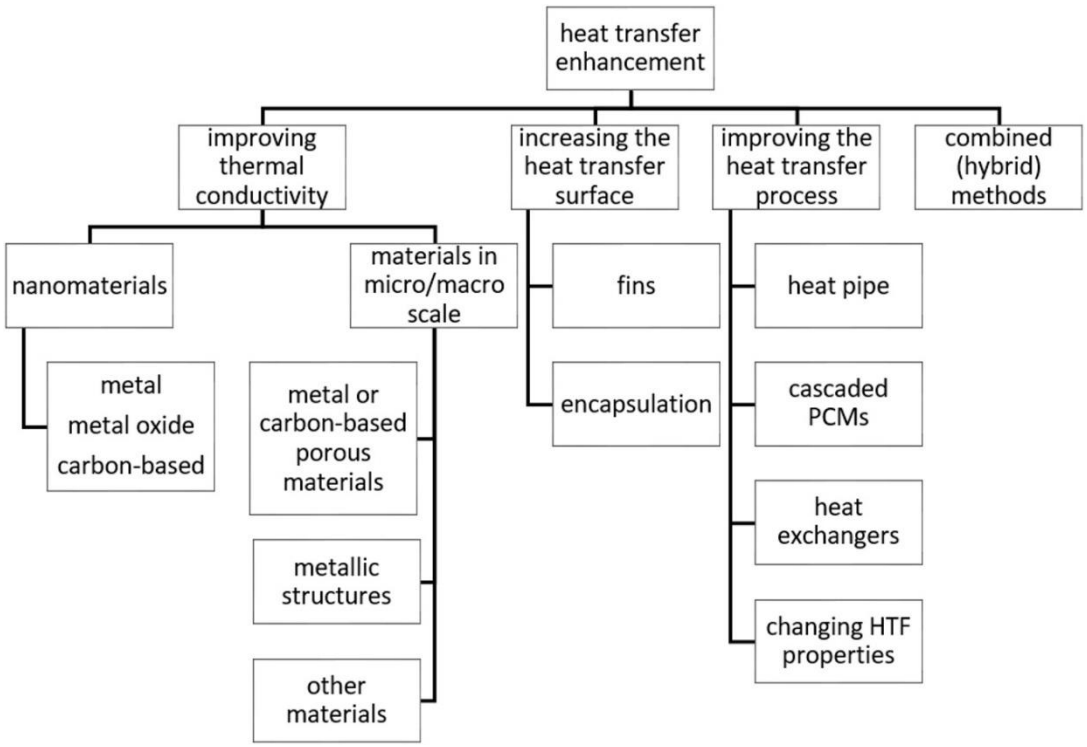

Figure 2. Classification of heat transfer enhancement techniques in latent heat thermal energy storage (LHTES).

In many cases, it is difficult to assign a heat transfer enhancement method in just one category since some techniques influence at least two parameters. For example, embedding PCMs into high thermal conductivity metal foam leads to both an increase in the effective thermal conductivity of composite material and an increase of the heat transfer surface area. In this paper, embedding PCMs into metal foam is included in improving the heat transfer conductivity group because most research on metal foam focuses only on thermal conductivity enhancement and neglects the fact of an increased heat transfer surface. A similar situation occurs in PCM encapsulation because encapsulated PCMs have a significant heat transfer surface area, and the shell of a capsule can be made of a high thermal conductivity material. Encapsulation is qualified for increasing the heat transfer surface method because shells are not always made of a high thermal conductivity material, but they always have an increased heat transfer surface area. Nevertheless, there is some research on encapsulation, which focuses on improving the thermal conductivity of shell materials, and such research is also discussed.

A detailed analysis of the mechanism of thermal conductivity enhancement of the enhanced PCMs can be found elsewhere [34]. Additionally, Liu et al. [35] and Rehman et al. [36] gathered the available correlations used to calculate the thermal conductivity of PCMs with thermal conductivity enhancers (TCEs).

There are several papers on heat transfer enhancement methods available in the literature [36–40]. Qureshi et al. [37] and Lin et al. [38] reviewed the addition of substances with high thermal conductivity and encapsulation as thermal conductivity enhancement techniques. Rehman et al. [36], in their work, focused only on using metallic and carbon-based porous materials to enhance thermal conductivity. Eanest Jebasingh and Arasu [39] and Leong et al. [40] reviewed research on nanoparticle insertion into PCMs. The abovementioned papers focus on either only one heat transfer enhancement technique or only thermal conductivity enhancement without considering how the applied method impacts other PCM properties. Therefore, there is a necessity to conduct a more comprehensive

analysis of the impact of TCEs on the main properties of PCMs, which has been carried out in this paper.

This paper aims to review, discuss, and compare the research carried out, mainly between 2010 and 2020, on the main properties of enhanced PCMs, including thermal conductivity, latent heat, melting temperature, specific heat, thermal and cycling stability. The main purpose of this paper is to review a possibly wide range of thermal conductivity enhancers types and their influence on the main properties of the most commonly used PCMs, however, without emphasizing the types, i.e., organic or inorganic, of the PCMs. The effect of encapsulation and addition of the high thermal conductivity materials on the nano-, micro-, and macro-scale into PCMs to improve the PCMs' properties is discussed. In each section, the influence of the TCEs on the thermal conductivity, latent heat, specific heat, melting temperature, and supercooling degree of the PCMs, as well as the other features, e.g., phase change time, or additional benefits of enhanced PCMs are discussed. Despite the numerous papers on heat transfer enhancement in LHTES, to the best of the authors' knowledge, none of them considers the impact of different TCEs on properties other than the thermal conductivity. Moreover, some missing information in the knowledge, as well as possible directions for further research, is pointed out. This is expected to give a more comprehensive insight into the impact of TCEs on PCMs' properties.

2. Nanomaterials

Nanomaterials, i.e., materials that possess at least one dimension less than 1 μm, have gained much attention in the scientific community since the past few decades. They have found an application in LHTES as well. Nanomaterials are added to PCMs to form composite nano-enhanced phase change materials (NEPCMs) with improved thermal conductivity. The following types of nanomaterials are used to prepare NEPCMs: metals, metal oxides, and carbon-based materials. Generally, their thermal conductivity is higher than the PCMs, and therefore they are treated as TCEs. Although nanomaterials can increase the thermal conductivity of PCMs, they also affect the other properties of the PCMs, which is overlooked in the vast majority of the papers. Therefore, there is a necessity to conduct a more complex analysis of the properties of NEPCMs, which has been undertaken in this paper.

Before discussing the properties of NEPCMs (or the other composite materials in Sections 3 and 4), it should be noted that the addition of nanomaterials (or the other thermal conductivity enhancers) into PCMs does not change the PCMs' intrinsic properties, e.g., thermal conductivity, latent heat, etc. because the chemical composition of the PCMs remains unchanged. However, composite PCMs can be treated as homogenous materials with effective properties, which means that the properties of such composite materials are somehow a combination of the properties of pure PCMs and additives. Therefore, each time properties of composite materials are presented in this paper, it is referred to as their effective properties.

Thermal conductivity, latent heat, and melting temperature of NEPCMs are usually investigated by the researchers. A summary of such results is shown in Table 2. Thermal conductivity enhancement was calculated according to Equation (2):

$$n = k_{eff}/k_{PCM}, \quad (2)$$

where n, k_{eff}, and k_{PCM} are the thermal conductivity enhancement, the thermal conductivity of NEPCMs, and the thermal conductivity of pure PCM, respectively. Generally, NEPCMs possess higher thermal conductivity than pure PCMs. Maximum improvement, up to 3.36 times, was obtained by Wang et al. [41], who added expanded graphite (EG) into the octanoic acid/myristic acid mixture. In the case of metal-based and metal oxide-based nanomaterials maximal improvement was 1.86 times for paraffin wax [42] and 1.79 times for paraffin wax [43], respectively. The improvement of thermal conductivity depends mainly on the mass or volume fraction of the nanomaterial added into a PCM (detailed data about the PCMs and their thermal conductivity enhancers discussed in this section are shown in Table 2). However, the results of the research on this issue are inconsistent. Some researchers indicated that the thermal conductivity increases linearly with increasing nanoparticles

fraction [44–48]. While others showed that the progression is nonlinear and the improvement starts to drop after reaching a certain value [42,49–53]. The results obtained by Soni et al. [44] are in the first group, but they were achieved by using numerical calculations. Hence, there is a necessity to conduct experimental studies to confirm the results. He et al. [54] found in their experimental investigation that the thermal conductivity of NEPCMs increased linearly in a liquid phase. In a solid state the improvement for nano-graphite (NG)/PCM was also linear, but for graphene nanoplatelets (GNP)/PCM and multi-walled carbon nanotubes (MWCNT)/PCM there was saturation tendency, caused by agglomeration or sedimentation of the nanoparticles. The agglomeration of the nanoparticles was also reported in [48,49,51,54]. As a result, the thermal conductivity of NEPCMs with high fraction of the nanoparticles started to decrease. Therefore, dispersion stabilizers are used, like: sodium stearoyl lactylate [43], sodium dodecyl benzene sulfonate [46], polyvinyl pyrrolidone [52,55], and oleoyl sarcosine [56]. Some studies [41,44,49,51,52,54,57] investigated the insertion of different types of the nanomaterials into one PCM. The results of [44,52,57] indicated that the thermal conductivity of NEPCMs increased with increasing thermal conductivity of the nanomaterials. On the other hand, the results obtained in [41,49,51,54] do not confirm the abovementioned one, because the thermal conductivity improvement was not the highest for the highest-thermal conductivity nanomaterial. This indicates, that the improvement depends not only on the thermal conductivity of the nanoparticles, but also on their effective concentration [49], the nature of fractal structures, aggregation dynamics, and variation in Kapitza resistance [51], as well as the method of preparation [56].

The second important parameter of the PCMs is latent heat, which might be influenced by nanoparticles addition. As a result of nanoparticles addition, a part of the PCM is replaced by the non-phase-changing material and less latent heat per NEPCM mass can be stored. Such phenomenon was confirmed by many researchers [41,42,44,46–48,54–56,58]. Based on Table 2, it can be concluded, that the decrease of the latent heat varied from about 2% to 15%, depending on the nanomaterial type and its mass fraction. The largest reduction of latent heat, by about 68%, was obtained by Ghossein et al. [56] who added silver nanoparticles (10 wt.%) into the eicosane. Theoretically, the latent heat of NEPCMs should decrease linearly with an increasing volume fraction of nanomaterials [41,44,46,55,56], which was confirmed experimentally by some researchers [41,47]. However, Masoumi et al. [46], Liu et al. [55], and Ghossein et al. [56] reported that the measured value of latent heat decreased more than predicted from the theory. According to Masoumi et al. [46], it was caused by the morphological, dimensional, and structural properties of the nanomaterials, while Ghossein et al. [56] attributed that finding to the colligative properties of the NEPCM.

On the other hand, the results on the latent heat of NEPCMs reported by some researchers [43,45,53,59] are significantly inconsistent with the abovementioned one, due to the fact that the NEPCMs' latent heat was higher than the latent heat of pure PCMs. Martin et al. [45] found that the latent heat of capric acid/SiO_2 and capric-myristic acid/SiO_2 increased by 8.0–10.7% and 6.8%, respectively, compared to pure PCM. Moreover, in the case of capric acid/SiO_2 the improvement was proportional to the SiO_2 mass fraction. Similar results were achieved by Zhu et al. [59], who prepared paraffin with aligned carbon nanotubes (a-CNT) and disordered carbon nanotubes (r-CNT). In the case of PCM/r-CNT the latent heat of NEPCM decreased, but for PCM/a-CNT an improvement by 11.2% was obtained, compared to pure PCM. The improvement of latent heat was proportional to the mass fraction of the nanoparticles. Vivekananthan and Amirtham [53] showed that the latent heat of melting increased from 311 kJ/kg to 338.6 kJ/kg, but the latent heat of solidification decreased from 308.2 kJ/kg to 252.8 kJ/kg for erythritol/GNP. Sami and Etesami [43] revealed that when the mass fraction of the TiO_2 increased to 3%, the latent heat of NEPCM also increased. However, further increasing the fraction of the TiO_2 resulted in decreased latent heat, compared to pure PCM. It was reported that increased latent heat of the NEPCM was caused by some interactions between nanoparticles and PCM molecules [43,59], however, it is not further discussed in this paper, and the readers are referred to [43,59] for details. Such abnormal results on latent heat like the abovementioned ones are in contrast with the findings reported previously in the literature and with

theoretical predictions. Therefore, it seems that they should be verified by retesting, and then possible explanations of such results could be given.

A more practical approach to investigate the thermal properties of NEPCMs is an analysis of their phase change time, which was reported in [41,44,52,57,60]. Phase change time of NEPCMs depends mainly on their thermal conductivity and latent heat. In the same operating conditions, the phase change time of NEPCMs will decrease with increasing thermal conductivity and decreasing latent heat, because of the two reasons. Firstly, as thermal conductivity increases, the heat is transferred into the PCM faster. Secondly, if the latent heat of material decreases, less heat is required to melt the PCM, thus, for constant heat flux, the PCM melting rate increases with decreasing latent heat. Soni et al. [44] numerically investigated the solidification time of the NEPCMs. In the first case of their study, they assumed that solidification is a conduction-dominated process, whereas in the second case, both conduction and convection were included. The solidification time for pure PCM in the first case was 18,150 s, while in the second case, it was 19,000 s. This shows that in the case of numerical investigations, the results obtained depend on the assumptions and the models used during calculations (e.g., the conduction or conduction-convection model of heat transfer). Therefore, each result obtained by numerical calculations should be checked experimentally. Nevertheless, in research carried out by Soni et al. [44], the solidification time of PCM with Cu, Al, SiO_2, and TiO_2 nanoparticles, including both convection and conduction, was shorter by 9.7%, 6.8%, 2.1%, and 5.2% respectively, compared to pure PCM. Prabakaran et al. [60] reported that the solidification time of PCM/GNP composite was reduced by 39.21%, compared to pure PCM. Similar results were obtained experimentally by Choi et al. [52], who concluded that the heat transfer rate during solidification increased with increasing concentration of graphite (average thickness of 5 μm), and graphene (average thickness of 7 nm) in the NEPCMs. However, in the case of MWCNT/PCM, the heat transfer rate started to decrease when the volume fraction of MWCNT was greater than 1%, due to the high viscosity of the NEPCM and slowed natural convection. Wang et al. [41] found experimentally that the solidification time of EG/PCM composite was 9.41 times shorter compared to pure PCM, but the melting time of NEPCM was longer than the pure PCM's, due to slowed natural convection. The opposite results were achieved by Gupta et al. [57], who investigated the melting and solidification time of Fe/PCM and Cu/PCM nanocomposites. Compared to pure PCM the melting time was reduced by 7.8% and 5.6% for Fe/PCM and Cu/PCM, respectively. The solidification time of Fe/PCM and Cu/PCM was reduced by 35% and 30%, respectively, compared to pure PCM. It is worth noting that despite the Cu/PCM had slightly higher thermal conductivity, its phase change time was longer than the Fe/PCM, although the nanoparticles fraction was equal in both cases.

Another property of NEPCMs, which influences the possibility of energy storage, is their specific heat. It should be noted that there are limited studies on this property. Soni et al. [44] found that the specific heat of NEPCM decreased linearly with increasing nanoparticle volume fraction. Moreover, the greatest decrease was noticed for copper nanoparticles (by 4.3%), while the smallest decrease was obtained for aluminum nanoparticles (by 3.3%) compared to the other nanoparticles analyzed by Soni et al. [44]. In contrast, Martin et al. [45] showed in experimental research that the specific heat of capric acid/SiO_2 and capric-myristic acid/SiO_2 increased by 19.0–22.0% and 20.4–23.5%, respectively, depending on the SiO_2 mass fraction. Similar findings were achieved by Aslfattahi et al. [58]. The specific heat of paraffin/Ti_3C_2 increased by 43% (compared to pure PCM) with an increasing mass fraction of the nanomaterial. According to the researchers it was caused by the interactions between the nanoparticles and the PCM.

The melting temperature of NEPCMs is generally only slightly different than the melting temperature of pure PCMs. Based on the information in Table 2, the abovementioned difference is less than 3 °C. In most cases, the melting temperature of NEPCM is a little lower than the pure PCM [41–43,46,47,55,56,59], but the opposite results can also be found [53,58]. Moreover, the nanoparticles can act as nucleating agents and decrease [42,48,53,55] or even eliminate [54] the supercooling degree, which is an advantage.

The next features of NEPCM are density and viscosity. These features are very rarely investigated by the researchers. Like was said in Section 1, a high density of PCMs is required,

especially when the volume of the LHTES system is limited [40]. Based on the numerical model Soni et al. [44] showed that the density of NEPCMs increased linearly with an increasing volume fraction of the nanoparticles. Compared to the pure PCM, from the four investigated NEPCMs the greatest increment of density (by 30%), and the smallest increment (by 2.5%) was obtained for Cu/PCM, and for Al/PCM, respectively. Viscosity influences the behavior of NEPCMs, for example, high viscosity might suppress natural convection during the melting process. The viscosity of NEPCMs increases as the mass fraction of the nanoparticles increases [45,50,60]. In studies carried out by Águila et al. [50] the viscosity of NEPCM increased by 61%, compared to pure PCM.

NEPCMs are expected to change their phase periodically in TES systems. Therefore, they should possess good cycling stability, which means that their properties should not change after many melting/solidification cycles. A slight decrease of the thermal conductivity [41,48,49,51], melting temperature [41,43,45,46,48,55], and latent heat [41,43,45,46,54,55,59] were observed after phase change cycles among the various literature reviewed. Martin et al. [45] showed that after 2000 cycles the latent heat of NEPCM decreased by 2.03%. Sami and Etesami [43] found that after 80 cycles the dispersion of the nanoparticles decreased. Nevertheless, some studies [48,53] confirmed that the changes in the properties of pure PCMs were higher than the changes of NEPCMs' properties. This confirms that the cycling stability of the NEPCMs can be better than pure PCMs. Ranjbar et al. [61] showed that after 500 cycles, the chemical structure of NEPCM did not change. It should be noted that among the reviewed literature, there are no chemical reactions in NEPCMs between the nanoparticles and the molecules of PCM [46,48,49,51,53–55,57,59,61].

Another benefit of NEPCMs can be their higher decomposition temperature, compared to pure PCM, which was proven by some researchers [42,43,45,46,58,59]. The decomposition temperature can be improved by 52 °C, which was obtained by Zhu et al. [59]. This indicates better thermal stability of the NEPCM than the pure PCMs. However, the opposite findings were also achieved [48,54], and the reduction of decomposition temperature might restrict potential applications of NEPCMs. On the other hand, some NEPCMs possess the ability to prevent PCM from leakage [59,61]. The lack of leakage means that the PCM after melting is still kept in the composite material and no loss of composite material's mass is observed. Such ability allows applying PCMs directly, for example, the NEPCMs without leakage can be placed directly on walls to maintain the constant temperature in the room, without the necessity of placing them into tanks or containers.

Nanomaterials are promising candidates for improving the properties of PCMs because they might provide many advantages. From the discussed literature in Section 2 and the data collected in Table 2, it can be concluded that nanomaterials can increase the thermal conductivity of PCMs about 3 times, but they decrease the latent heat, and generally, the latent heat of NEPCMs decreases with increasing thermal conductivity. Nevertheless, nanomaterials can decrease or even eliminate the supercooling degree, improve thermal stability, and cycling stability. However, there are still some issues to be investigated. Firstly, there is a lack of complex studies that investigate all the properties of NEPCMs. Most of them focus only on one aspect, mainly the thermal conductivity, and the other properties are neglected, while the fact of decreased latent heat (usually up to 15%) of the NEPCMs, which was found in the majority of research, seems to be crucial in LHTES systems. Latent heat determines heat storage density, and therefore the optimum between thermal conductivity enhancement and latent heat reduction has to be found. However, the cases in which the latent and sensible heat of NEPCMs was improved require further studies to explain such results. Most of the researchers do not investigate the phase change time of NEPCMs. Like it was said before, increased thermal conductivity not always leads to the faster melting process. In many cases, researchers presented the value of thermal conductivity in one state only and/or they did not specify if the given value refers to the liquid or solid state of the material. Furthermore, sometimes researchers reported only the value of thermal conductivity enhancement, but they did not explain how they calculated it. For example, Mishra et al. [51] defined the thermal conductivity enhancement as:

$$n = [(k_{eff}-k_{PCM})/k_{PCM}]\cdot 100\%, \quad (3)$$

where n, k_{eff}, and k_{PCM} are the thermal conductivity enhancement, the thermal conductivity of NEPCMs, and the thermal conductivity of pure PCMs, respectively, but in [45] the thermal conductivity enhancement was calculated as:

$$n = (k_{eff} - k_{PCM}) \cdot 100\%, \quad (4)$$

With n, k_{eff}, and k_{PCM} as before. There are also some problems with agglomeration and/or sedimentation of the nanoparticles. Solving this issue could be the subject of further studies. Additionally, the cost of the NEPCMs is overlooked. Only Mishra et al. [51] suggested that carbon black nano-powder (CBNP) might be one of the best candidates to be a TCE, due to its relatively low price of $1/g, compared to MWCNT, single-walled carbon nanotubes, and EG price of $5/g, $75/g, and $100/g, respectively. Martin et al. [45] suggested that the price of NEPCMs is high and there is a necessity to develop low-cost NEPCMs production methods on a large scale.

Table 2. Properties of nano-enhanced phase change materials (NEPCMs).

Reference	PCM	Additive	Additive Fraction	Melting Temperature, (°C)		Latent Heat, (kJ/kg)		Thermal Conductivity (W/(m·K)) [1]		Maximum Thermal Conductivity Enhancement, (Times)	
				PCM	NEPCM	PCM	NEPCM	PCM	Additive	Liquid	Solid
Sami and Etesami [43]	Paraffin [4]	TiO_2	3 wt.%	58.9	56.0	137.8	167	0.08 (l) 0.147 (s)	n.a.	1.79	1.34
Lin and Al-Kayiem [42]	Paraffin wax [4]	Cu	2.0 wt.%	60.42	57.81	184.2	157.3	0.172	401	1.86 [3]	
Ali et al. [47]	Paraffin wax [4]	Nano graphene	3 wt.%	29.83	28.12	230.08	216.10	0.123 (l) 0.185 (s)	n.a.	2.46	n.a.
Aslfattahi et al. [58]	Paraffin wax [4]	Ti_3C_2	0.3 wt.%	69.8	71.7	110.68	99.53	0.197 (s)	n.a.	1.16 [3]	
Zhu et al. [59]	Paraffin wax [4]	a-CNT	7 wt.%	47.36–58.84	46.72–57.02	196.47	218.56	0.24	n.a.	n.a.	2.33
		r-CNT	15 wt.%		45.82–56.84		174.12		n.a.	n.a.	n.a.
Ranjbar et al. [61]	N-heptadecane	SiO_2	33.3 wt.%	n.a.	25.6	n.a.	123.8	0.1662	n.a.	1.71 [3]	n.a.
		EG	7 wt.%		6.8		136.3		300	3.36	n.a.
Águila et al. [50]	Octadecane	CuO	10 w/v.%	28–30	n.a.	n.a.	n.a.	0.131 (l) 0.147 (s)	18	n.a.	1.09
Ghossein et al. [56]	Eicosane	Ag	10 wt.%	36.4	33.5	241	78.3	n.a.	n.a.	n.a.	1.32
Vivekananthan and Amirtham [53]	Erythritol	GNP	1 wt.%	127.52	120.01	311.00	338.60	0.326 (l) 0.733 (s)	n.a.	n.a.	1.53
Soni et al. [44]	Erythritol	Cu	2.5 vol.%	118	n.a.	339.8	288.8	0.326 (l) 0.733 (s)	400	1.0767	1.0765
		Al	2.5 vol.%		n.a.		322.7		237	1.0766	1.0762
		SiO_2	2.5 vol.%		n.a.		325.7		1.38	1.0394	1.0172
		TiO_2	2.5 vol.%		n.a.		322.1		8.4	1.0684	1.0594
Salyan and Suresh [48]	D-mannitol	CuO	0.5 wt.%	166.38–168.38	165.76–168.76	281.89	273.20	1.308(s)	n.a.	n.a.	1.25

Wang et al. [41]	Octanoic acid/myristic acid	MWCNT	0.01 wt.%	7.13	n.a.	146.1	n.a.	0.2971 (l)	2000–6000	1.23	n.a.
		EG	7 wt.%		6.8		136.3		300	3.36	n.a.
Martín et al. [45]	Capric acid	SiO_2	1.5 wt.%	31.5	31.2	150	166	0.296 (l)	n.a.	1.79	n.a.
	Capric acid/myristic acid	SiO_2	1.5 wt.%	21.9	22.1	148	158	n.a.	n.a.	1.42	n.a.
He et al. [54]	Myristic acid	GNP	3 wt.%	54–55	54.3	194.90	187.19	0.1846 (l) 0.2186 (s)	n.a.	1.60	2.76
		MWCNT	3 wt.%		54.4		188.47		n.a.	1.13	1.47
		NG	3 wt.%		54.6		188.90		n.a.	1.12	1.44
Mishra et al. [51]	Palmitic acid/dimethyl formamide	Al_2O_3	2 vol.%	36	n.a.	25	n.a.	0.162 (l) 0.196 (s)	35	1.17	1.59
		GNP	2 vol.%		n.a.		n.a.		3000	1.24	1.95
		MWCNT	1.5 vol.%		n.a.		n.a.		6600	1.18	1.72
Masoumi et al. [46]	Stearic acid	CBNP	4 vol.%	62–64	n.a.	134	n.a.	0.15 (l) 0.20 (s)	0.182	1.12	3.05
		TiO_2	0.36 wt.%		61.6–63.6		130.5		n.a.	1.07	1.175
Choi et al. [52]	Stearic acid	MWCNT	0.1 vol.%	64–71	n.a.	203	n.a.	0.17 (l) 0.33 (s)	3000	1.015	n.a.
		Graphite	0.1 vol.%		n.a.		n.a.		200	1.099	n.a.
		Graphene	0.1 vol.%		n.a.		n.a.		5000	1.215	n.a.
Prabakaran et al. [60]	Fatty acid-based OM08	GNP	0.5 vol.%	8–9	n.a.	180	n.a.	0.168 (l) 0.235 (s)	n.a.	1.46	2.02
Liu et al. [55]	$KAl(SO_4)_2{\cdot}12H_2O/Na_2SO_4{\cdot}10H_2O$	Nanocarbon	1 wt.%	67.03	65.68	135.7	132.2	0.546 (s)	n.a.	n.a.	1.67
Gupta et al. [57]	Magnesium nitrate hexahydrate	Fe	0.5 wt.%	n.a.	n.a.	n.a.	n.a.	0.4 (s)	n.a.	n.a.	1.525
		Cu	0.5 wt.%		n.a.		n.a.		n.a.	n.a.	1.575
Mishra et al. [49]	Phenol-water mixture	Al_2O_3	4 wt.%	24.5	n.a.	n.a.	n.a.	0.170 (l) 0.195 (s)	35	1.070	1.412
		SiO_2	2/3 wt.%		n.a.		n.a.		1.4	1.041	1.382
		HP-SiO_2 [2]	1/3 wt.%		n.a.		n.a.		1.4	1.024	1.265
		TiO_2	4/3 wt.%		n.a.		n.a.		15	1.094	1.382
		Al_2O_3+CBNP	4 + 0.04 wt.%		n.a.		n.a.		35 + n.a.	1.076	1.459
		SiO_2+CBNP	3 + 0.04 wt.%		n.a.		n.a.		1.4 + n.a.	1.041	1.453
		TiO_2+CBNP	3 + 0.02 wt.%		n.a.		n.a.		15 + n.a.	1.088	1.412

[1] (l)—thermal conductivity in a liquid state; (s)—thermal conductivity in a solid state. [2] SiO_2—hydrophilic; HP-SiO_2—hydrophobic. [3] The author did not specify the state in which thermal conductivity was measured. [4] No compositional details are given by the sources. n.a.—not available.

3. Materials at Micro- and Macro Scales

The second type of materials, which can be used to increase the thermal conductivity of PCMs, are materials at micro- and/or macro-scales. Their sizes are greater than or equal to 1 μm and usually, they do not exceed a few millimeters [62]. To enhance the thermal performance of LHTES, the following materials were investigated: metal-based porous materials [63–75] or other metallic structures [72,76], carbon fibers [62,77–79], carbon-based porous materials [78,80–88], and other materials [59,89–93]. PCMs with insertions in the micro/macro-scale create composite phase change materials (CPCMs). In some cases, the thermal properties of CPCM were not investigated, but instead, the thermal performance of a TES system containing the composite material was examined. The results of such research are shown in Table 3, in which the melting and/or solidification time improvement was calculated as:

$$t_{imp} = (t_{PCM} - t_{CPCM})/t_{PCM} \cdot 100\%, \quad (5)$$

where t_{imp}, t_{PCM}, and t_{CPMC} are melting (or solidification) time improvement, melting (or solidification) time of pure PCMs, and melting (or solidification) time of CPCMs, respectively. The research that investigated the thermal properties of CPCMs is summarized in Table 4, in which the thermal conductivity improvement was calculated according to Equation (2).

Some experimental research showed that the thermal conductivity of paraffin, KNO_3-$LiNO_3$-$Ca(NO_3)_2$, and paraffin wax can be increased about 25 times [77], 50 times [80], and 45 times [63], when the carbon fibers, EG, and copper foam were added into the abovementioned PCMs, respectively. Wang et al. [64] estimated that the thermal conductivity of PCM/aluminum foam was 220 times higher than the pure PCM's. However, this value was calculated theoretically, and this prediction was not confirmed experimentally. Similarly, Fleming et al. [68] used a semi-analytical approach to estimate the thermal conductivity of PCM/aluminum foam composite.

The thermal conductivity of a CPCM depends on a few factors, mainly on the type and a mass or volume fraction of an additive. Various research showed that the thermal conductivity of CPCMs increases linearly with an increasing fraction of additive [62,78,80–83,89]. However, numerous studies concluded that the abovementioned relation was nonlinear [69,78,79], and the thermal conductivity enhancement showed a saturation tendency [84–86], which means that the increase in the thermal conductivity was getting smaller as the fraction of additives increased. Nevertheless, based on the literature reviewed, it seems that the linear relation between the thermal conductivity enhancement and the fraction of TCE was observed mainly for carbon-based porous materials, although the non-linear relation for these materials was also reported. Therefore, it seems that the available results of investigations are insufficient to make general conclusions on this issue.

Secondly, the features of an additive may play an important role in thermal conductivity enhancement. The influence of carbon fibers' length was studied in [62,77,79]. Fukai et al. [77] showed that the influence of carbon fibers' length on the thermal conductivity improvement was insignificant, but the arrangement of carbon fibers was crucial. The fibers in the form of brush performed about 4 times better in terms of thermal conductivity enhancement than the fibers in the random arrangement. Frusteri et al. [62] found that the shortest carbon fibers ensured the highest thermal conductivity enhancement because their distribution in the PCM was the most homogenous. On the other hand, Zhang et al. [79] showed that longer carbon fibers resulted in greater thermal conductivity enhancement than the shorter ones. However, it should be noted that in [62,77] the length of the fibers was in the order of millimeters (the most advantageous length of carbon fibers was 0.2 mm [62]), while in [79] in the order of micrometers (the most advantageous length of carbon fibers was 0.225 mm [79]). Therefore, according to these studies, the carbon fibers' length of 0.2 mm seems to be optimal for thermal conductivity enhancement.

When porous materials are used to improve the properties of PCMs, porosity and pore density might affect the properties of CPCMs. According to [63,64,67–69] porosity is the ratio of the volume of pores to the total volume of a material, usually given in percentages. Pore density, measured in pores per inch (PPI), can be defined as the number of pores in one linear inch. Usually, thermal conductivity improvement is inversely proportional to the porosity of porous materials

[63,67,68,70,90]. In research conducted by Li et al. [67], the thermal conductivity of CPCM increased from 3.3 W/(m·K) to 6.8 W/(m·K) when the porosity of copper foam decreased from 97.3% to 92.4%. In research conducted by Zheng and Wang [70], the thermal conductivity of PCM/copper foam was 1.22 W/(m·K) and 7.07 W/(m·K) for the porosity of copper foam 98% and 93%, respectively. Xiao et al. [63] found that when the porosity of copper foam decreased from 96.95% to 88.89%, the thermal conductivity of CPCM increased from 5.04 W/(m·K) to 16.01 W/(m·K), and when the porosity of nickel foam decreased from 97.45% to 90.61%, the thermal conductivity of CPCM increased from 1.24 W/(m·K) to 2.33 W/(m·K). Li et al. [90] showed that reduction of the porosity of porous ceramics from 90% to 67% resulted in the improvement of thermal conductivity from 0.30 W/(m·K) to 0.51 W/(m·K). However, the results of research on the influence of pore density on the thermal conductivity enhancement are more inconsistent. Huang et al. [66] concluded that the thermal conductivity of CPCM decreased with increasing pore density of the copper, as well as nickel foam. On the contrary, Zhu et al. [71] found that as the pore density of iron foam increased, the thermal conductivity of CPCM also increased. Xiao et al. [63] concluded that the pore density did not affect significantly thermal conductivity improvement. Due to the inconsistency of the abovementioned results of experimental investigations, it is difficult to conclude unambiguously what effect the pore density has on the thermal conductivity enhancement. However, it seems that there should be an optimal pore density for which the thermal conductivity improvement is the greatest. Moreover, the measured value of the thermal conductivity of composite materials depends, among others, on the homogeneity of a tested sample, and the homogeneity of composite materials may vary significantly depending on porosity or pore density. Therefore, this issue could be a subject for further studies. Other features of materials that might affect the properties of CPCMs are the particle size of the material and its density. Two research teams found that thermal conductivity enhancement was greater when the size of TCE particles was smaller [84,91]. Additionally, Li et al. [91] concluded that thermal conductivity improvement was inversely proportional to the density of MgO, and the maximum thermal conductivity of CPCM was 5.81 W/(m·K). On the other hand, the opposite relation was found by Xiao et al. [86].

In addition to the abovementioned features of additives, the properties of CPCMs depend as well on the method of preparation [78] and a form of the prepared composite material [87]. Cheng et al. [78] used tetradecanol as PCM, expanded perlite (EP) as shape-stabilizing material, and copper powder, or carbon fibers as TCEs. From these materials, they prepared CPCMs by two different methods: mixing and implanting. In the mixing method, the TD and copper powder (or carbon fibers) were physically mixed, and then impregnated into the EP, whereas in the implanting method, the copper powder (or carbon fibers) were firstly implanted (added) into the EP and then the TD was impregnated into the previously prepared composite (copper powder (or carbon fibers)-EP). The results showed that the mixing method gave a better performance in terms of controllability and thermal conductivity enhancement compared to the implanting method. Ren et al. [87] made two CPCMs from $Ca(NO_3)_2$-$NaNO_3$ and EG: one in granular form, and second in a shape-stable form prepared in cold compression and sintering process. The thermal conductivity of CPCM in the shape-stable form was much higher (5.02–6.27 W/(m·K)) than in the granular form (1.56–1.90 W/(m·K)). Such phenomenon was the result of better connections between the particles of materials caused by the shape-stabilization process. To further improve the thermal conductivity of PCMs, some scientists proposed adding simultaneously two (or more) types of TCEs into one PCM. For example: iron foam and GNP [71], MgO and graphite flakes [91], high-density polyethylene (HDPE) and EG and MWCNT (or carbon nanofibers (CNF)) [88,94], and mullite and graphite flakes [92]. The combination of two or more thermal conductivity enhancers provides a synergistic thermal conductivity enhancement effect [88,94].

The main goal of inserting high thermal conductivity materials into PCMs is to increase the thermal conductivity of PCMs and hence to improve heat transfer rate and reduce charging (melting) or discharging (solidification) time. However, it should be noted that different researchers might define the charging and/or discharging time differently. For example, Yang et al. [72] defined the charging time as the time after which all PCM mass will be melted, but Liu et al. [73] and Righetti et

al. [69] defined the charging time as the time after which temperature inside the LHTES unit will achieve a set value, i.e., the temperature set above the melting (or below the solidification in case of discharging) temperature of PCM. Moreover, the range of initial and end temperature of the PCM can be different in various research. Such discrepancies might make it difficult to compare the results obtained by different scientists. Therefore, the results given below in this paragraph are not compared to each other. Nevertheless, it has been proven in many experimental studies that inserting high thermal conductivity materials into PCMs results in shorter melting [63,66,68–70,76,78,84,86–89], and/or solidification time [69,73,74,77,80,81,83,88,89,92]. For example, the addition of copper, and alumina foam can decrease the melting time by 76.8% [74], and 93.6% [69], respectively, compared to pure PCM. The solidification time can be decreased by 72.2% [74] and 88.3% [69] for copper and alumina foam, respectively. Xu et al. [75] found that the melting time of PCM/copper foam can be reduced by 86.2%, but this result was obtained by numerical calculations. Hence, that finding should be checked experimentally. When TiO_2 was added into n-octadecane, the melting and solidification time decreased by 45% and 26%, respectively [89]. Qu et al. [88] found that adding TCEs resulted in reduced melting and solidification time by 8.9–54.6% and 8.9–42.7% respectively, compared to pure PCM. The addition of EG can reduce the melting time by 73% [82]. These results indicate that the addition of the abovementioned inserts influences more the melting time than solidification time. However, Fu et al. [81] showed that the solidification time of the EG/PCM composite was reduced more than the melting time. A possible explanation for these discrepancies could be the different nature of the melting and solidification process, in which the convection and conduction are the dominant heat transfer mechanism, respectively. In the works discussed above in this paragraph, the different PCMs and TCEs were used, thus their thermophysical properties were different, which could affect the heat transfer, for example, it could suppress natural convection (as in the [81]).

Like was mentioned before, in the case of the metal foams application, thermal conductivity enhancement depends on their porosity and pore density. Righetti et al. [69] concluded that the pore density did not affect phase change time, but the melting and solidification time decreased with decreasing porosity of aluminum foam, which is consistent with the statement of the inversely proportional relationship between the porosity and thermal conductivity enhancement. The same result was reported by Chen et al. [74]. In contrast, Xu et al. [75] showed that the melting time of copper foam/PCM decreased with increasing porosity of the foam.

Although in the vast majority of research, phase change time of the CPCM decreases as its thermal conductivity increases, Fukai et al. [77] obtained different results. They found that the melting time of the CPCM with the volume fraction of carbon fibers less than 1% was longer compared to pure PCM. The reason for such a result was suppressed natural convection by the carbon fibers. Only when the volume fraction of the fibers increased to 2% the melting time of CPCM was the same as the pure PCM, because conduction heat transfer increased, and it compensated suppressed natural convection. On the other hand, the solidification time decreased with increasing volume fraction of the fibers. In addition to the already mentioned materials, the addition of other structures, like metallic meshes [95], aluminum honeycomb structures [96], aluminum or carbon fins [97] into PCMs can also be found in the literature. Another benefit of inserting high thermal conductivity materials into PCMs is a more uniform temperature distribution in the LHTES units [64,67,69,72,73].

The next desired property of LHTES systems is large heat storage capacity, which is directly related to latent heat and specific heat of the CPCMs. Based on data in Table 4 it can be concluded that the latent heat of CPCM is lower than the latent heat of pure PCMs. The decrease of a latent heat varies in a range of 1.4% [84] to 83.5% [89], depending on the type and fraction of additive. The latent heat of CPCMs decreases with increasing mass fraction of the additive [61,66,67–71,74,75,81,84,86]. The specific heat of CPCMs is very rarely investigated by researchers. Xiao et al. [68] found that the specific heat of CPCMs decreased in both solid and liquid phases by 14.8–23.5% and 13.5–21.7%, respectively, compared to pure PCM. This was because the specific heat of additive was lower than pure PCM. On the other hand, Qu et al. [88] found that the specific heat of CPCMs in the liquid state

decreased by 4.7–12.6%, but the specific heat in the solid state increased by 4.5%, compared to pure PCM.

Regarding the latent heat and the specific heat, some researchers investigated a more practical aspect, i.e., the heat storage capacity of LHTES units. Frusteri et al. [62] showed that the total heat storage capacity in the temperature range of 20–70 °C for pure PCM and CPCM was 292 kJ/L and 270 kJ/L, respectively. According to Liu et al. [73], the total heat storage capacity of the LHTES unit with CPCM increased by 3.1%, compared to the unit with pure PCM. Such improvement was caused by sensible heat stored in the metal foam. A similar result was obtained by Yang et al. [72]. It should be noted, that the results reported by Liu et al. [73] and Yang et al. [72] are possible only when the sensible heat stored in TCE is larger than the latent heat lost due to reduced mass of PCM.

The second practical aspect investigated by the researchers is the heat transfer rate, which can be improved by using CPCMs instead of pure PCMs [73,75,76]. In the LHTES system investigated by Liu et al. [73], the heat transfer rate increased by 49.3% and 10% during melting and solidification, respectively. Comprehensive numerical investigation of the LHTES with PCM locally enhanced with copper foam (Figure 3) was conducted by Xu et al. [75]. It was concluded that to achieve the lowest melting time simultaneously maintaining the heat storage capacity value of the LHTES system as high as possible (by reducing the mass of TCE), foam inserts should be gathered in the lower part of the annular region (Figure 3a). Compared to a case in (Figure 3d), the average heat transfer rate increased to 5.1, 6.8, and 6.9 times for cases (Figure 3a), (Figure 3b), and (Figure 3c), respectively, but the heat storage capacity per unit mass decreased to 0.93, 0.86, and 0.81 times for cases (Figure 3a), (Figure 3b), and (Figure 3c), respectively. Although the best thermal performance in terms of melting time and heat transfer rate was achieved by the LHTES unit filled with metal foam/PCM (Figure 3c), the units with PCM locally enhanced (cases (Figure 3a) and (Figure 3b)) might reduce the costs of metal foam. This is consistent with the conclusion made by Gasia et al. [76], who investigated four heat exchangers with: pure PCM, 17 aluminum fins, metallic wool distributed in a finned shape around the HTF tubes, and metallic wool distributed randomly around the HTF tubes. It was concluded that although the heat exchanger with fins gave the best performance, the advantage of metallic wool is its availability and low price. Lu et al. [80] estimated that the cost of CPCM consisted of KNO_3-$LiNO_3$-$Ca(NO_3)_2$ and expanded graphite (EG) was lower than the pure PCM, because the price of EG was lower than the price of PCM. Nevertheless, a majority of researchers neglect the cost of CPCMs.

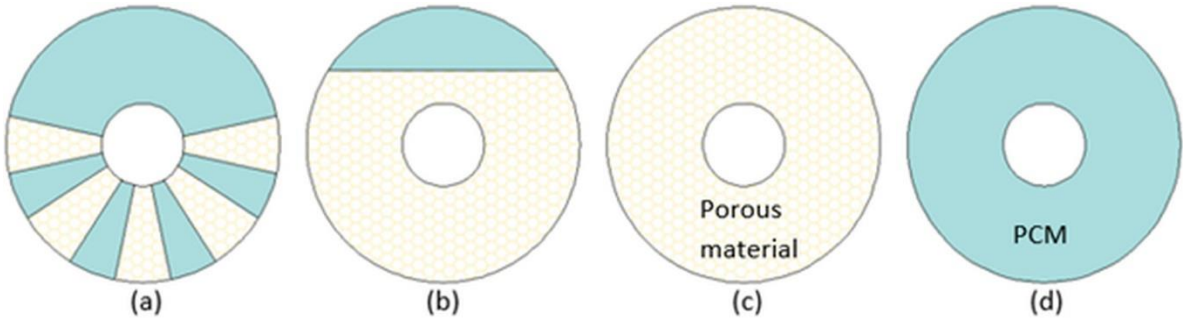

Figure 3. A cross-section of LHTES units with (**a**) porous inserts, (**b**) partially filled LHTES with metal foam, (**c**) LHTES with PCM/metal foam composite, (**d**) LHTES with PCM only [75].

Phase change temperature is another important property of composite PCMs with inserts at micro/macro-scale, which defines their application suitability. Based on data in Table 4, it can be concluded that in most cases the melting temperature of CPCMs decreases slightly, by less than 4 °C [78,80,81,83–85,89,90], which is an acceptable change. Nevertheless, much more reduction of melting temperature, by 18 °C, was also observed [82]. In some studies [66,68,71,79,88] a slight increase, from 0.96 °C [68] to 1.9 °C [79], of the melting temperature was detected. Usually, the changes in melting temperatures were independent of the mass or volume fraction of additive. However, some researchers found that the changes in melting temperatures were proportional to the fraction of

additives [78], especially when the EG was used as TCE [80,82,83]. Different types of MgO (light and heavy, with densities of 0.2 g/mL and 0.5 g/mL, respectively) were used by Li et al. [91], who found that the melting temperature of CPCM with light and heavy MgO decreased by 3–5 °C and 6–9 °C, respectively, compared to pure PCM. Kenisarin et al. [84] used two types of EG with different sizes: 200–1200 μm and 50–200 μm. The melting temperature of CPCMs with large EG size, and with small EG size decreased by 1 °C, and 7–8 °C, respectively, compared to pure PCM. According to Kenisarin et al. [84], that difference was caused by some intermolecular interactions between PCM and the smaller EG. It should be noted, that only Kenisarin et al. [84] discovered some intermolecular interactions between the PCM and the additive. According to the authors, the nature of these interactions should be further investigated. The vast majority of the research found that PCMs and additives are physically mixed and no chemical reactions occur among them [57,61,66–72,74,75,79,81,83,86].

Another advantage of CPCMs is their reduced supercooling degree, compared to pure PCMs [85,86,89,92]. For example, in research conducted by Xiao et al. [86] the supercooling degree was reduced from 13 °C (pure PCM) to 2.4 °C (composite PCM). The supercooling degree of CPCMs prepared by Qu et al. [88] was only 0.1 °C, but the researchers did not give the value of the supercooling degree for pure PCM. Fu et al. [81] and Yuan et al. [82] found that a larger reduction of supercooling degrees can be obtained by increasing the mass fraction of additive. On the other hand, Huang et al. [66] showed that the supercooling degree increased from 0.51 °C for pure PCM, to 2.75–3.50 °C for CPCMs with copper, and nickel foam. A similar finding was obtained by Xiao et al. [68].

The properties of CPCMs should not change after many melting-solidification cycles, which means that they should possess good cycling stability. Generally, after numerous melting/solidification cycles of the CPCMs listed in Table 4, their latent heat decreased [59,78,81,84–86,89,90,92] in the range from 0.7% [78] to 19% [84] after 200 phase change cycles. The changes in melting temperature were usually referred to as negligibly small [78,81,84–86,92]. However, Xiao et al. [86] found that the supercooling degree of CPCM increased after 400 melting-solidification cycles, but its value was still below 5 °C. Additionally, Li et al. [90] found that after 25 cycles the weight loss of CPCM was less than 10%, which indicated leakage of the PCM. A small leakage, i.e., the CPCM's mass decreased by 1.38%, of the PCM after 40 cycles was reported also by Yuan et al. [82]. Furthermore, Li et al. [91] observed a breakage of graphite flakes in the CPCM after 100 cycles.

Additives at micro/macro-scales should not impact the thermal stability of CPCMs, especially they should not reduce a decomposition temperature. Some studies confirmed that there were no noticeable changes in the decomposition temperature of CPCMs, compared to pure PCMs [66,71,83,85,89,91,92]. For example, the decomposition temperature of CPCM prepared by Cheng et al. [78] decreased by 2.9 °C, compared to pure PCM. It could be concluded, that such small change does not influence the working temperature range of CPCMs.

Adding materials at micro/macro-scale into PCMs has also an operational advantage. It can prevent PCMs from leakage due to the possibility of preparing shape-stable composite materials [57,66,68–70,74,79,82–84,86,95]. Depending on the type of additive, different mass fractions of additives must be used to prevent PCM from leakage. Yuan et al. [82], Zhang et al. [85], and Zhu et al. [59] prepared the erythritol/EG, n-eicosane/EG/SiO_2, and paraffin wax/expanded vermiculite composite materials, respectively, and the maximum mass fractions of PCMs in these composite materials were 90%, 70%, and 60%, respectively. If the mass fractions of PCMs in the CPCMs exceeded the abovementioned values, a leakage of PCMs occurred. Another interesting property that CPCMs might possess is flexibility, which was reported by Wu et al. [83]. They prepared the flexible CPCM using paraffin wax, olefin block copolymer (OBC) and EG. Such flexible CPCM may considerably extend the scope of CPCMs use. On the other hand, the use of porous ceramics as TCE allowed preparing CPCMs with high mechanical strength [90,91].

Summarizing, the application of additives at micro/micro-scales can provide many benefits. Firstly, it can significantly (up to 50 times) improve the thermal conductivity of PCMs, and as a result, shorten phase change time (up to 93.6%). However, some studies proved that the additives may suppress natural convection during melting and therefore extend phase change time. It should be

noted that the phase change time was not always investigated by researchers. Moreover, the charging/discharging time was defined differently by different researchers, which makes it difficult to compare. Another advantage of CPCMs is that they provide more uniform temperature distribution in LHTES units, and they possess good thermal and cycling stability. Generally, melting temperatures of CPCMs are very similar to those of pure PCMs, while the supercooling degree of CPCMs might be reduced and reach value as low as 0.1 °C. Additionally, the additives can prevent PCMs from leakage. On the other hand, the main negative effect of using additives at micro/macro-scales is decreased latent heat of CPCMs (up to 83.5%). Hence, the heat storage density of a LHTES unit might be reduced. However, some studies showed that the heat storage density of a TES unit with CPCM might be higher compared to a unit with pure PCM, because of specific heat stored in the additive. The next important feature of CPCMs is their cost, which is overlooked by most of the researchers. Therefore, it can be generally concluded that there is a lack of studies that investigate every aspect of preparing CPCMs and all their most important properties.

Table 3. Performances of LHTESs with PCMs enhanced with materials at micro/macro-scales.

Reference	PCM			Additive				Type of Heat Exchanger/Thermal Storage Unit	Maximum Improvement, (%)	
	Type	Latent Heat, (kJ/kg)	Thermal Conductivity, (W/(m·K)) [1]	Type	Porosity, (%)	Pore Density, (PPI)	Thermal Conductivity, (W/(m·K))		Melting Time	Solidification Time
Yang et al. [72]	Paraffin wax [4]	250	0.125 (l) 0.301 (s)	Copper foam	96.8	20	400	Shell-and-tube; vertical	36	n.a.
Liu et al. [73]	Paraffin [4]	170.4	0.21 (l, s)	Copper foam	93	10	n.a.	Rectangular box with U-shape heating tube	47.6	8.3
Chen et al. [74]	Paraffin RT 58	181	0.2	Copper foam	90	10	387.6	Plate heat exchanger	76.8	72.2
Righetti et al. [69]	RT40	165	0.21 (l, s)	Alumina foams: [2]				Vertical tubes in a water bath		
				I	92.1	5	170		93.0	80.8
				II	89.3	10	170		93.6	88.3
				III	92.7	10	170		90.3	83.3
				IV	94.8	10	170		88.6	79.2
				V	92.7	20	170		91.3	84.2
				VI	91.4	40	170		91.3	82.5
				Alumina periodic structure [3]	92	n.a.	n.a.		63.0	37.5
Gasia et al. [76]	N-octadecane	243.5	0.148 (l) 0.190 (s)	Rectangular aluminum fins	-	-	n.a.	LHTES based on the shell-and-tube heat exchangers	n.a.	n.a.
				Metallic wool	-	-	n.a.		n.a.	n.a.
				Metallic wool (arbitrarily)	-	-	n.a.		n.a.	n.a.
Xu et al. [75]	Li_2CO_3-K_2CO_3	342	0.6	Copper foam	95	10	350	Horizontal shell-and-tube	86.2	n.a.

[1] (l)—thermal conductivity in a liquid state; (s)—thermal conductivity in a solid state. [2] The numbers I–VI includes the alumina foams with porosities and pore densities given in the columns Porosity and Pore density. [3] Alumina periodic structure is alumina net rolled in a cylindrical shape. [4] No compositional details are given by the sources. n.a.—not available.

Table 4. Properties of PCMs enhanced with materials at micro/macro-scales.

Reference	PCM	Additive	Additive Fraction	Additive Characteristics	Melting Temperature, (°C)		Latent Heat, (kJ/kg)		Thermal Conductivity (W/(m·K)) [1]		Maximum Thermal Conductivity Enhancement, (Times)	
					PCM	CPCM	PCM	CPCM	PCM	Additive	Liquid	Solid
Fukai et al. [77]	Paraffin wax [6]	Carbon fiber	2 vol.%	Diameter: 10 μm Length: 5 mm	41–43	n.a.	n.a.	n.a.	0.26 (s)	220	n.a.	6 (random) 25 (brush)
Zhu et al. [59]	Paraffin wax [6]	Expanded vermiculite	40 wt.%	n.a.	47.36–58.84	46.79–56.77	196.47	119.42	0.24	n.a.	n.a.	n.a.
Kenisarin et al. [84]	Paraffin wax [6]	Expandable graphite	6 wt.% 6 wt.%	(200–1200) μm (50–200) μm	49–61	48–60 45–50	143.78	136.03 141.82	0.258 (s)	n.a. n.a.	2.11 3.02	3.79 4.90
Li et al. [90]	Paraffin wax [6]	Tailing porous ceramics	n.a.	Porosity: 71% Pore density: n.a.	50.3	49.9	196.0	71.1	0.25 (s)	1.41	n.a.	1.8
Wu et al. [83]	Paraffin wax [6]	OBC + EG	18 + 10 wt.%	n.a.	51.43	47.42	200.6	176.7	0.45	n.a.	12.22 [2]	
Zheng and Wang [70]	Paraffin [6]	Copper foam	n.a.	Porosity: 93% Pore density: 10 PPI	48–50	n.a.	220	n.a.	0.26	398	27.19 [2]	
Xiao et al. [68]	Paraffin [6]	Nickel foam	n.a.	Porosity: >95% Pore density: 5 PPI	52.10	52.70	189.4	144.4	0.305 (s)	91.4	n.a.	3.93
		Copper foam	n.a.	Porosity: >95% Pore density: 10 PPI		53.06		135.2		398	n.a.	16.07
Xiao et al. [63]	Paraffin [6]	Nickel foam	n.a.	Porosity: 90.61% Pore density: 25 PPI	n.a.	n.a.	n.a.	n.a.	0.354	91.4	6.58 [2]	
		Copper foam	n.a.	Porosity: 88.89% Pore density: n.a.		n.a.		n.a.		398	45.22 [2]	
Wang et al. [64]	Paraffin [6]	Aluminum foam	n.a.	Porosity: 78.95% Pore density: n.a.	n.a.	n.a.	n.a.	n.a.	0.21 (l) 0.29 (s)	218	219.24 [3]	159.03 [3]
Qu et al. [88]	N-octadecane	HDPE	20 wt.%	EG granularity: 75 μm MWCNT:	28.2	28.8	239.4	189.0	0.25	0.4	1.12 [2]	

		HDPE-EG/MWCNT	20–4/1 wt.%	Diameter: <8 nm Length: (10–20) μm CNF:	28.2	29.1	239.4	170.5	0.25	0.4–3000/1950		5.44 [2]
		HDPE-EG/CNF	20–4/1 wt.%	Diameter: (200–600) nm Length: (5–50) μm		28.2		168.4		0.4–3000/1150		4.12 [2]
Li et al. [89]	N-octadecane	Porous TiO_2	70 wt.%	Pore size: 15.8 nm	28.4	27.8	267.4	44.2	0.16	n.a.		2.81 [2]
Chen et al. [93]	N-octadecane	Carbonized wood + graphite coating	n.a.	n.a.	28	n.a.	239.9	209.1	0.28 (s)	0.46 + n.a.	n.a.	2.43
Zhang et al. [85]	N-eicosane	EG + SiO_2	7 + 30 wt.%	EG thickness: (5–20) nm EG flake diameter: (5–10) μm SiO_2 particle size: 20 nm	36.90–38.78	35.35–37.71	243.28	135.80	0.145 (s)	n.a.	n.a.	2.30
Cheng et al. [78]	Tetradecanol	Copper powder	n.a.	n.a.	36.6	35.8	203.5	199.8	0.481 (s)	400	n.a.	3.30
		Carbon fiber	n.a.	n.a.		n.a.		n.a		400–450	n.a.	3.36
		EP	77.7 wt.%	n.a.		36.4		158.2		0.047–0.07	n.a.	0.96
		Copper powder + EP	n.a.	n.a.		35.5		156.7		-	n.a.	3.04
		Carbon fiber + EP	n.a.	n.a.		34.6		155.4		-	n.a.	3.13
Huang et al. [66]	Myristyl alcohol	Copper foam	44.6 wt.%	Porosity: n.a. Pore density: 40 PPI	38.29	39.61	218.4	201.39	0.1701	n.a.	n.a.	8.54
		Nickel foam	16.7 wt.%	Porosity: n.a. Pore density: 40 PPI		39.55		211.53		n.a.	n.a.	2.80
Yuan et al. [82]	Erythritol	EG	15 wt.%	n.a.	116–132	98–125	244.4	198.3	0.72 (s)	n.a.	n.a.	20.85
Zhang et al. [79]	Erythritol	Carbon fiber	10 wt.%	Diameter: 9 μm Length: 40 μm	116.3	n.a.	385.3	n.a.	0.77 (s)	900	n.a.	3.19

				225 μm		118.2		340.4		900	n.a.	5.08
Zhu et al. [71]	Lauric acid	Iron foam	30.9 wt.%	Porosity: n.a Pore density: 90 PPI	45.52	46.58	179.44	102.03	0.115	0.528	9.31 [2]	
		Iron foam+GNP	28.6 + 3 wt.%	GNP thickness: (5–20) nm		46.08		95.17		n.a.	10.67 [2]	
Gu et al. [92]	Palmitic acid	Mullite	70 wt.%	n.a.	66.11	64.75	213.10	54.70	0.28 (s)	n.a.	n.a.	1.14
		Mullite + graphite powder	70 wt.% + 5 wt.%	n.a.		n.a.		52.30		n.a.	n.a.	1.86
Frusteri et al. [62]	PCM44 (inorganic mixture)	Carbon fiber	10 wt.%	Diameter: 6 μm Length: 0.2 mm	44	n.a.	n.a.	n.a.	0.47 (s)	175–200	n.a.	4.25
				3 mm		n.a.		n.a.		175–200	n.a.	3.53
				6 mm		n.a.		n.a.		175–200	n.a.	3.87
Fleming et al. [65]	Water	Aluminum foam	n.a.	Pore density: 40 PPI	n.a.	n.a.	333	315[3)]	0.6 (l) 2.25 (s)	n.a.	3.00 [3]	2.27 [3]
Li et al. [91]	$NaLiCO_3$	MgO + graphite flakes	n.a. + 35 wt.%	Light MgO particle size: (3–5) μm	500.35	n.a.	347.9	n.a.	n.a.	n.a.	n.a.	n.a.
Xiao et al. [86]	$Ba(OH)_2 \cdot 8H_2O$	MEG	15 wt.%	Matrix density: 200 g/l	78.3	77.8	256.4	238.4	n.a.	n.a.	1.84 [2]	
Ren et al. [87]	$Ca(NO_3)_2$-$NaNO_3$ [4]	EG	7 wt.%	n.a.	218.15–286.9	217.6–285.6	185.85	169.17	0.56	n.a.	3.39 [2]	
	$Ca(NO_3)_2$-$NaNO_3$ [5]				222.8–237.1	216.6–267.3	88.77	82.44	0.46	n.a.	13.63 [2]	
Lu et al. [80]	KNO_3-$LiNO_3$-$Ca(NO_3)_2$	EG	30 wt.%	n.a.	116.8	115.2	131.8	89.6	0.44	n.a.	49.75 [2]	
Fu et al. [81]	SAT-urea mixture	EG	12 wt.%	n.a.	50.82	48.84	240.4	199.1	0.6785 (s)	n.a.	n.a.	4.13
Li et al. [67]	SAT + DHPD	Copper foam	n.a.	Porosity: 92.4% Pore density: 15 PPI	57–58	n.a.	258	n.a.	n.a.	398	11 [2]	

[1] (l)—thermal conductivity in a liquid state; (s)—thermal conductivity in a solid state. [2] The authors did not specify the state in which thermal conductivity was measured. [3] Estimated theoretical value. [4] Mole fraction of $Ca(NO_3)_2$ was 0.1, a composite material in the granular form. [5] Mole fraction of $Ca(NO_3)_2$ was 0.5, a composite material in the shape-stable form. [6] No compositional details are given by the sources. n.a.—not available.

4. Encapsulation

Heat storage in PCMs is connected with the melting process, and therefore, the presence of materials in a liquid state is inevitable. Hence, there is a necessity of locating PCMs in enclosures to prevent the material from leakage. One possible solution to the problem of leakage is the encapsulation of PCMs. In the literature, there are different definitions of encapsulation—for some researchers, encapsulation means a tank of any shape and size filled with PCMs, but for others, a capsule is a spherical shell with a PCM core, and this approach is the most commonly used [98]. Depending on the size, PCM capsules have been divided into three groups: macrocapsules, microcapsules, and nanocapsules, wherein dimensions of these capsules are more than 1 mm (but usually less than 10 cm), 1 μm–1 mm, and less than 1 μm, respectively [98]. PCM capsules, besides the fact that they prevent material from leakage, they have another advantage—a possibility to disperse them in liquid, e.g., water, to create PCM slurries, which can accumulate the heat and transfer the heat [99]. Usually, the heat capacity of such heat transfer fluids (HTFs), i.e., PCM slurries, is much greater compared to HTFs that use only sensible heat; furthermore, the thermal conductivity of PCM slurries may be higher than the thermal conductivity of HTFs that uses only sensible heat [100].

As mentioned in Section 1, encapsulation has been classified as one of the heat transfer enhancement techniques, mainly due to the large heat transfer surface area of capsules [101,102]. Nevertheless, the capsules' shells can be made of high thermal conductivity materials, which lead to the greater thermal conductivity of the whole capsule. Studies on encapsulation that focus on the high thermal conductivity shells are summarized in Table 5. The thermal conductivity of capsules can be improved up to 11 times, which was reported by Yu et al. [103], who prepared the capsule made of n-octadecane (core) and $CaCO_3$ (shell). The improvement of thermal conductivity depends, among others, on the mass fraction of shell. If the thermal conductivity of shell is higher than the thermal conductivity of PCM, then the thermal conductivity of capsules increases with an increasing shell to core mass ratio [103,104]. The second factor that affects the thermal conductivity of the PCM capsule is a type of shell material and some of the researchers proposed to create hybrid shells [100,105–107]. Such hybrid shells consist of at least two different materials. Xia et al. [106] fabricated the capsule with a melamine-formaldehyde (MF)/boron nitrate (BN) hybrid shell. The thermal conductivity of capsule increased almost linearly with increasing mass fraction of BN. Similar findings were obtained by Wang et al. [107], who created the capsules with the shell made of poly(melamine-formaldehyde) (PMF) and different mass fraction of SiC. Although the thermal conductivity of capsules increased with increasing fraction of SiC, some aggregates in the products occurred when SiC content increased to 7 wt.%. However, the application of SiC resulted in additional benefit, i.e., increased solar irradiation absorbance. As a result, the temperature of the hybrid-shell capsule was higher by 8 °C compared to the single-shell capsule after exposure to sunlight due to photo-thermal conversion. Such property could be utilized in solar energy applications. The capsules prepared by Zhu et al. [100] possessed the same property (photo-thermal conversion). The capsules were made of SiO_2/graphene shells with different graphene mass fractions. Moreover, the thermal conductivity of capsules increased to about 1.5 W/(m·K) as graphene mass fraction increased to 2.5%. However, when graphene concentration further increased to 3.75 wt.%, and 5.0 wt.% the thermal conductivity of capsules decreased to 0.99 W/(m·K), and 0.97 W/(m·K), respectively. According to the authors, this abnormal phenomenon was caused by differences in the capsules' sizes, i.e., the size of the capsules with graphene mass fraction of 2.5%, 3.75%, and 5.0% was 390 nm, 257 nm, and 256 nm, respectively. Hybrid shells were also prepared by Zhu et al. [105]. The shells consisted of polystyrene (PS) and SiO_2 or poly (hydroxyethyl methacrylate) (PHEMA) and SiO_2. The capsules with PS/SiO_2, and PHEMA/SiO_2 shells possessed higher thermal conductivity than the capsules with SiO_2 shell, which, according to Zhu et al. [105], was inconsistent with their predictions because the organic materials (PS and PHEMA) possessed lower thermal conductivities than inorganic material (SiO_2). The researchers explained that result by a unique, more compact structure of the hybrid shells. Moreover, the mechanical properties of capsules with hybrid shells were superior compared to capsules' with SiO_2 shell. Another way of capsules thermal conductivity enhancement

was proposed by Praveen et al. [108], who did not create a hybrid shell, but mixed GNP with capsules. As a result, voids between the microcapsules were filled with GNP, which improved the heat transfer.

Increased thermal conductivity of capsules should reduce the phase change time of PCMs, which was examined by some researchers [98,101,104,105,107]. The charging and discharging time of capsules prepared by Zhang et al. [102] was reduced by 6.4%, and 29.4%, respectively, compared to pure PCM. Zhu et al. [105] found that the charging time of PCM/PS/SiO_2, and PCM/PHEMA/SiO_2 capsules was reduced by 23.4%, and 18.0%, respectively, compared to PCM/SiO_2 capsule. The charging time reduction obtained by Wang et al. [107] was 11.9%, while the greatest charging time reduction, by 54.4%, was achieved by Zhu et al. [100].

The other method of phase change time reduction was proposed by Jia et al. [109], who investigated numerically the solidification process in the capsule with circular pin-fins, as shown in Figure 4. It was found that increasing the number of fins, their length, and diameter led to a reduction of solidification time by 60%. However, the reduction was insignificant after the number of fins, their length, and diameter exceeded 6, 15 mm, and 2 mm, respectively. Moreover, such operations resulted in decreased PCM mass by about 1.5%. Puertas et al. [110] used numerical simulations to examine the influence of the capsule's thermal conductivity on the melting time of PCM. They found that the melting time decreased by 20% when the thermal conductivity of the capsule increased 100 times. Similarly, Feng et al. [111] compared the phase change time of PCMs placed in tubular capsules with different thermal conductivities. It was concluded that the thermal conductivity of shell had a minor impact on the phase change time than the thermal conductivity of PCMs. Therefore, increasing the thermal conductivity of PCMs seems to be more advantageous than increasing the thermal conductivity of shells.

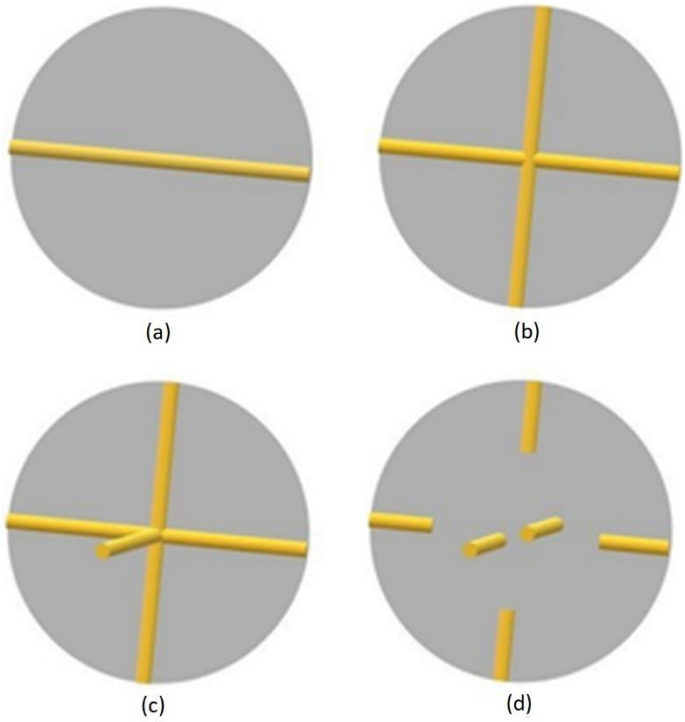

Figure 4. Spherical capsules with: (**a**) two circular pin-fins, (**b**) four circular pin-fins, (**c**) six circular pin-fins, (**d**) six circular pin-fins with reduced length to radius ratio [109].

Praveen et al. [108] investigated the thermal performance of heat sink without PCM (case I), with pure PCM (case II), and with capsules (case III). The heat was supplied to the heat sink until its (heat sink) temperature rose to 80 °C and it was assumed that the longer time to reach this temperature, the better was the thermal performance of the heat sink. It was found that the time to reach 80 °C was about 50 min, 88 min, and 62 min for cases I, II, and III, respectively. Therefore, despite the PCM capsules had higher thermal conductivity than pure PCM, their thermal performance was worse,

because of lower latent heat. The low latent heat of PCM capsules is their main drawback. Based on information from Table 5, it can be concluded that in most cases the latent heat of PCM capsules decreased by approximately 30–50% [100,102,105–108,112], compared to pure PCMs. However, the smallest and the largest reduction were 15.5% [104] and 77.6% [103], respectively. The latent heat reduction depends mainly on the core to shell mass ratio, and the latent heat decreases with decreasing value of that ratio [102–104,105,112]. However, Zhu et al. [100], Wang et al. [107], and Xia et al. [106] found that there is no relationship between the mass fraction of shell and the latent heat of capsule. Moreover, Xia et al. [106] showed that the increase of boron nitrate (BN) mass fraction in shell resulted in higher latent heat, compared to the capsule with shell made of only melamine-formaldehyde (MF). According to the authors, that phenomenon was a result of increased thermal conductivity of the capsule which allowed the entire mass of PCM to change its phase.

Another property of encapsulated PCMs is their melting temperature. Generally, changes in capsules' melting temperatures are negligibly small, less than 1 °C [102–104,106–108,112]. However, in two studies [100,105] the melting temperature of capsules decreased by about 3 °C, independently from the shell to the core mass ratio. Additionally, the shell material can act as a nucleating agent, hence reduce the supercooling degree [100,103,107,112]. In contrast, Zhu et al. [105] obtained different results that indicated extended supercooling for capsules.

Some of the researchers investigated the thermal stability of PCM capsules and changes in their properties after melting-solidification cycles i.e., cycling stability. Zhu et al. [100], Yu et al. [103], and Cheng et al. [104] did not observe significant changes in the melting temperature and latent heat of capsules after 500, 200, and 20 melting/solidification cycles, respectively. Only slight fluctuations in the melting temperature and the latent heat of capsule were detected by Xia et al. [106], after 40 cycles. However, some of the studies showed that the latent heat of capsules decreased by 9% [105], and 19.7% [102] after 100 and 500 cycles, respectively. Regarding the thermal stability, it was determined, that encapsulation did not influence the thermal stability and decomposition temperature [102,105,108,112]. Moreover, in some studies [100,103,106,107], the decomposition temperature increased, because shell acted as a protective barrier. It should be noted that encapsulation does not change the crystal structure of the encapsulated PCM [100,102,105,112], and no chemical reactions between the core and shell materials occur [106,107].

Summarizing, PCMs' encapsulation might bring considerable benefits. It prevents PCMs from leakage and gives the possibility to prepare PCMs slurries, which can store, as well as transport heat. Generally, capsules filled with PCMs possess good thermal and cycling stability. Their melting temperature is comparable to that of pure PCMs, while a supercooling degree can be reduced. Their thermal conductivity can be 11 times higher than PCMs. Nevertheless, their main disadvantage is low latent heat, reduced by about 80% in comparison with pure PCM. On the other hand, the specific heat of capsules, as well as the cost of capsules preparation was overlooked by the researchers. Moreover, n-octadecane was a core material in the majority of the studies. Hence, there is an opportunity for researchers to create and investigate the properties of capsules with other types of PCMs as core materials.

Table 5. Properties of encapsulated PCMs.

Reference	Core-PCM	Shell	Capsule Size	Melting Temperature, (°C)		Latent Heat, (kJ/kg)		Thermal Conductivity (W/(m·K)) [1]			Maximum Thermal Conductivity Enhancement, (Times)	
				PCM	Capsule	PCM	Capsule	PCM	Shell	Capsule	Liquid	Solid
Praveen et al. [108]	Paraffin [3]	Polyurethane	(60–65) μm	60–62	62.31	211.93	116.71	n.a.	n.a.	0.192	n.a.	n.a.
		Polyurethane + GNP	(60–65) μm		62.71		110.71		n.a.	0.379	n.a.	1.97 (compared to PCM/ polyurethane)
Cheng et al. [104]	Paraffin wax ($C_{26}H_{54}$)	VO_2	(5–15) μm (average 8 μm)	58.71	58.22	193	163	0.28	4–6	1.53	5.46 [2]	
Zhu et al. [100]	N-octadecane	SiO_2	440 nm	30.5	28.31	202.0	109.7	n.a.	n.a.	0.6416 (s)	n.a.	n.a.
		SiO_2 + 2.5 wt.% of graphene	390 nm		27.72		108.2		n.a.	1.4941 (s)	n.a.	n.a.
Yu et al. [103]	N-octadecane	$CaCO_3$	5 μm	28.74	28.09	209.10	46.93	0.153	2.467	1.674	10.94 [2]	
Zhu et al. [105]	N-octadecane	SiO_2	335 nm	30.5	27.5	202.0	108.6	0.153 (s)	n.a.	0.3332	n.a.	2.18
		PS-SiO_2	303 nm		28.1		86.1		n.a.	0.3844	n.a.	2.51
		PHEMA-SiO_2	449 nm		27.9		104.3		n.a.	0.3823	n.a.	2.50
Xia et al. [106]	N-octadecane	MF	(5–10) μm	26.4	26.2	205.4	125.9	n.a.	n.a.	0.084	n.a.	n.a.
		MF-BN 0.5 g	(5–10) μm		26.1		131.2		n.a.	0.109	n.a.	1.2976 (compared to PCM/MF)
Wang et al. [107]	N-octadecane	PMF	3 μm	29.9	29.8	250.6	173.0	n.a.	n.a.	n.a.	n.a.	n.a.
		PMF-SiC 7 wt.%	n.a.		29.5		168.0		n.a.	n.a.	1.60 (compared to PCM/PMF) [2]	
Zhang et al. [112]	N-octadecane	Silica	8.76 μm	26.7	26.9	214.6	123.0	0.1505 (s)	1.2960	0.6213	n.a.	4.13
Zhong et al. [101]	NaCl	Graphite	60 mm	808	n.a.	294	n.a.	0.40 (s)	28.01–31.55	n.a.	n.a.	n.a.
	NaCl + graphite + cellulose	Graphite	60 mm	803	n.a.	159.6	n.a.	13.93 (s)		n.a.	n.a.	n.a.
Zhang et al. [102]	$Na_2SO_4 \cdot 10H_2O$	SiO_2	500 nm	33.7	33.6	211.9	125.6	n.a.	n.a.	n.a.	n.a.	n.a.

[1] (l)—thermal conductivity in a liquid state; (s)—thermal conductivity in a solid state. [2] The authors did not specify the state in which thermal conductivity was measured. [3] No compositional details are given by the sources. n.a.—not available.

5. Conclusions

In this paper, the research available in the open literature from 2010 to 2020 on the influence of TCEs on the properties of PCMs has been reviewed. The impact of various nanomaterials like: metals, metal oxides, and carbon-based nanoparticles has been studied. The addition of materials at the micro- and macro-scale such as carbon fibers, metal foams, expanded graphite, and the other materials have been also investigated. Additionally, the properties of encapsulated PCMs have been presented.

All of the TCEs might impact significantly the properties of PCMs. The properties depend on the type of TCE, its mass or volume fraction, as well as its physical properties like shape or size. A preparation method of enhanced PCMs is also important. Nevertheless, the TCEs can improve the thermal conductivity of PCMs. The greatest improvement (up to 50 times) can be achieved by using materials at the micro/macro-scale. PCMs encapsulation can improve the thermal conductivity up to 11 times. The lowest improvement is provided by nanomaterials (about 3 times). However, to achieve the same thermal conductivity improvement, up to 3 times, a much smaller mass fraction of the nanoparticles is required than the materials at micro/macro-scale. The reduction of the TCE amount leads to a lower decrease in latent heat. Therefore, the latent heat reduction of NEPCMs (up to 15%) is much lower than CPCMs (up to 83.5%) and capsules (up to 77.6%). Moreover, in some cases, the latent heat and the specific heat of NEPCMs was higher than pure PCMs which should be further investigated, because the reason for this phenomenon has not been thoroughly explained.

The addition of TCEs leads to higher thermal conductivity values, but some studies showed that it might be not enough to shorten the phase change time of PCMs, because TCEs may suppress natural convection. Therefore, the mass or volume fraction of the added materials should be chosen very carefully. However, in the majority of studies phase change time of enhanced PCMs was reduced, compared to pure PCMs. Scientists attributed it to the improved thermal conductivity, but it should be noted that decreased latent heat might also contribute to reduced phase change time.

Generally, melting temperatures of NEPCMs, CPCMs, and capsules undergo minor changes, while the TCEs or shells can act like nucleating agents, which reduces the supercooling degree. Enhanced PCMs possess good thermal and cycling stability, which means that their properties do not change after many thermal cycles. Moreover, the thermal stability of enhanced PCMs can be even improved. Another benefit of capsules is preventing PCMs from leakage and the possibility of preparing PCMs slurries, which possess the ability to store and transport heat. CPCMs can also prevent PCMs from leakage, and they allow to create shape-stable or flexible materials. Furthermore, the temperature distribution in TES units with CPCMs is more uniform than in units with pure PCMs.

Although researchers dedicate much effort to improve the thermal conductivity of PCMs, knowledge is still incomplete. Many issues should be investigated and could be the subject of future work. Many researchers focus only on thermal conductivity enhancement, and they do not investigate the influence of additives on other PCM properties. Furthermore, most of the research concerns organic PCMs with low melting temperatures (below 130 °C). Therefore, more inorganic PCMs and PCMs with higher melting temperatures should be investigated, and further research should include the influence of additives on all of the properties of enhanced PCMs. The economic aspect of preparing enhanced PCMs is also neglected. The influence of shape, size, and geometry of additives on properties of enhanced PCMs is not fully explored, and therefore requires more research. In most research the thermal conductivity of enhanced PCMs is measured. However, the time of phase change should also be investigated because some additives can suppress the natural convection, and despite increased thermal conductivity, the phase change time may be increased. Moreover, there is not enough comprehensive research that would cover the impact of TCEs on all of the properties of PCMs such as thermal conductivity, latent heat, specific heat, melting temperature, thermal stability, cycling stability, and its influence on the performance of LHTES units.

Based on the presented work, it can be concluded that although the greatest improvement of the thermal conductivity can be achieved by using TCEs at the micro/macro-scale and PCMs encapsulation, these additives and encapsulation may reduce the latent heat such significantly, that

the CPCMs or PCM capsules will not fulfil their role as thermal energy storage materials. Moreover, the use of such composite materials could be associated with application problems, i.e., the necessity of creating thermal energy storage tanks with large volume and mass, which is unfavorable. Therefore, the addition of nanoparticles seems to be the most promising technique to improve PCMs' properties. A low nanoparticle mass fraction can considerably improve thermal conductivity with a relatively small decrease of latent heat. On the other hand, preparing shape-stable PCMs also seems to be a prospective direction of development because they do not require special tanks or containers, they can be made in any shape, and there are even attempts to create flexible ones, which can significantly expand the possibilities of their applications. Nevertheless, research on the preparing NEPCMs and shape-stable PCMs is relatively new, but this area of research is developing, and the number of studies on the NEPCMs and shape-stable PCMs is increasing every year. Therefore, this direction of research seems to be the most promising.

Author Contributions: The contribution of co-authors in creating the article is: conceptualization, E.R.; writing—original draft preparation, E.R.; writing—review and editing, L.M. and K.S.; supervision, L.M. and K.S.; funding acquisition, L.M. All authors have read and agreed to the published version of the manuscript.

Funding: This research received no external funding.

Acknowledgments: This research was funded by a subsidy from the Faculty of Energy and Fuels AGH University of Science and Technology number 16.16.210.476.

Conflicts of Interest: The authors declare no conflict of interest.

Nomenclature

A	surface area, m^2
k	thermal conductivity, W/(m·K)
n	thermal conductivity improvement, -
$\dot{Q}$	heat transfer rate, W
t	time, h
t_{imp}	melting (solidification) time improvement, %
U	heat transfer coefficient, W/m^2
ΔT	temperature difference, °C, K

Abbreviations

a-CNT	aligned carbon nanotubes
CBNP	carbon black nano-powder
CNF	carbon nanofibers
CPCM	composite phase change material
DHPD	disodium hydrogen phosphate dodecahydrate ($Na_2HPO_4 \cdot 12H_2O$)
EG	expanded graphite
EP	expanded perlite
GNP	graphene nanoplatelets
HDPE	high-density polyethylene
HTF	heat transfer fluid
LHTES	latent heat thermal energy storage
MEG	modified expanded graphite
MF	melamine-formaldehyde
Mtoe	million tons of oil equivalent
MWCNT	multi-walled carbon nanotubes
NEPCM	nano-enhanced phase change material
NG	nano-graphite
OBC	olefin block copolymer
PCM	phase change material
PHEMA	poly (hydroxyethyl methacrylate)

PMF	poly(melamine-formaldehyde)
PS	polystyrene
PPI	pores per inch
r-CNT	disordered carbon nanotubes
RES	renewable energy sources
SAT	sodium acetate trihydrate ($CH_3COONa{\cdot}3H_2O$)
STES	sensible thermal energy storage
TCE	thermal conductivity enhancer
TES	thermal energy storage
TPES	total primary energy supply

Subscripts

CPCM	composite phase change material
eff	effective
PCM	phase change material

References

1. International Energy Agency. *World Energy Balances: An Overview*; International Energy Agency: Paris, France, 2019.
2. Koohi-Fayegh, S.; Rosen, M.A. A review of energy storage types, applications and recent developments. *J. Energy Storage* **2020**, *27*, doi:10.1016/j.est.2019.101047.
3. Tatsidjodoung, P.; Le Pierrès, N.; Luo, L. A review of potential materials for thermal energy storage in building applications. *Renew. Sustain. Energy Rev.* **2013**, *18*, 327–349, doi:10.1016/j.rser.2012.10.025.
4. Nazir, H.; Batool, M.; Bolivar Osorio, F.J.; Isaza-Ruiz, M.; Xu, X.; Vignarooban, K.; Phelan, P.; Inamuddin; Kannan, A.M. Recent developments in phase change materials for energy storage applications: A review. *Int. J. Heat Mass Transf.* **2019**, *129*, 491–523, doi:10.1016/j.ijheatmasstransfer.2018.09.126.
5. Yan, T.; Wang, R.Z.; Li, T.X.; Wang, L.W.; Fred, I.T. A review of promising candidate reactions for chemical heat storage. *Renew. Sustain. Energy Rev.* **2015**, *43*, 13–31, doi:10.1016/j.rser.2014.11.015.
6. Scapino, L.; Zondag, H.A.; Van Bael, J.; Diriken, J.; Rindt, C.C.M. Sorption heat storage for long-term low-temperature applications: A review on the advancements at material and prototype scale. *Appl. Energy* **2017**, *190*, 920–948, doi:10.1016/j.apenergy.2016.12.148.
7. Lizana, J.; Chacartegui, R.; Barrios-Padura, A.; Valverde, J.M. Advances in thermal energy storage materials and their applications towards zero energy buildings: A critical review. *Appl. Energy* **2017**, *203*, 219–239, doi:10.1016/j.apenergy.2017.06.008.
8. Alva, G.; Lin, Y.; Fang, G. An overview of thermal energy storage systems. *Energy* **2018**, *144*, 341–378, doi:10.1016/j.energy.2017.12.037.
9. Lott, M.C.; Kim, S.I.; Tam, C.; Houssin, D.; Gagné, J.F. *Technology Roadmap: Energy Storage*; International Energy Agency (IEA): Paris, France, 2014.
10. Sharma, A.; Tyagi, V.V.; Chen, C.R.; Buddhi, D. Review on thermal energy storage with phase change materials and applications. *Renew. Sustain. Energy Rev.* **2009**, *13*, 318–345, doi:10.1016/j.rser.2007.10.005.
11. Elias, C.N.; Stathopoulos, V.N. A comprehensive review of recent advances in materials aspects of phase change materials in thermal energy storage. *Energy Procedia* **2019**, *161*, 385–394, doi:10.1016/j.egypro.2019.02.101.
12. Zalba, B.; Marín, J.M.; Cabeza, L.F.; Mehling, H. Review on thermal energy storage with phase change: Materials, heat transfer analysis and applications. *Appl. Therm. Eng.* **2003**, *23*, 251–283, doi:10.1016/S1359-4311(02)00192-8.
13. Fallahi, A.; Guldentops, G.; Tao, M.; Granados-Focil, S.; Van Dessel, S. Review on solid–solid phase change materials for thermal energy storage: Molecular structure and thermal properties. *Appl. Therm. Eng.* **2017**, *127*, 1427–1441.
14. Abhat, A. Low temperature latent heat thermal energy storage: Heat storage materials. *Sol. Energy* **1983**, *30*, 313–332, doi:10.1016/0038-092X(83)90186-X.

15. Mohamed, S.A.; Al-Sulaiman, F.A.; Ibrahim, N.I.; Zahir, M.H.; Al-Ahmed, A.; Saidur, R.; Yılbaş, B.S.; Sahin, A.Z. A review on current status and challenges of inorganic phase change materials for thermal energy storage systems. *Renew. Sustain. Energy Rev.* **2017**, *70*, 1072–1089, doi:10.1016/j.rser.2016.12.012.
16. Mathis, D.; Blanchet, P.; Lagière, P.; Landry, V. Performance of Wood-Based Panels Integrated with a Bio-Based Phase Change Material: A Full-Scale Experiment in a Cold Climate with Timber-Frame Huts. *Energies* **2018**, *11*, 3093, doi:10.3390/en11113093.
17. Li, D.; Wang, J.; Ding, Y.; Yao, H.; Huang, Y. Dynamic thermal management for industrial waste heat recovery based on phase change material thermal storage. *Appl. Energy* **2019**, *236*, 1168–1182, doi:10.1016/j.apenergy.2018.12.040.
18. Abdelsalam, M.Y.; Teamah, H.M.; Lightstone, M.F.; Cotton, J.S. Hybrid thermal energy storage with phase change materials for solar domestic hot water applications: Direct versus indirect heat exchange systems. *Renew. Energy* **2020**, *147*, 77–88, doi:10.1016/j.renene.2019.08.121.
19. Siahkamari, L.; Rahimi, M.; Azimi, N.; Banibayat, M. Experimental investigation on using a novel phase change material (PCM) in micro structure photovoltaic cooling system. *Int. Commun. Heat Mass Transf.* **2019**, *100*, 60–66, doi:10.1016/j.icheatmasstransfer.2018.12.020.
20. Guerraiche, D.; Bougriou, C.; Guerraiche, K.; Valenzuela, L.; Driss, Z. Experimental and numerical study of a solar collector using phase change material as heat storage. *J. Energy Storage* **2020**, *27*, 101133, doi:10.1016/j.est.2019.101133.
21. Mofijur, M.; Mahlia, T.M.I.; Silitonga, A.S.; Ong, H.C.; Silakhori, M.; Hasan, M.H.; Putra, N.; Ashrafur Rahman, S.M. Phase Change Materials (PCM) for Solar Energy Usages and Storage: An Overview. *Energies* **2019**, *12*, 3167.
22. Jiang, Z.Y.; Qu, Z.G. Lithium–ion battery thermal management using heat pipe and phase change material during discharge–charge cycle: A comprehensive numerical study. *Appl. Energy* **2019**, *242*, 378–392, doi:10.1016/j.apenergy.2019.03.043.
23. Ganatra, Y.; Ruiz, J.; Howarter, J.A.; Marconnet, A. Experimental investigation of Phase Change Materials for thermal management of handheld devices. *Int. J. Therm. Sci.* **2018**, *129*, 358–364, doi:10.1016/j.ijthermalsci.2018.03.012.
24. Iqbal, K.; Sun, D. Development of thermo-regulating polypropylene fibre containing microencapsulated phase change materials. *Renew. Energy* **2014**, *71*, 473–479, doi:10.1016/j.renene.2014.05.063.
25. Said, M.A.; Hassan, H. Parametric study on the effect of using cold thermal storage energy of phase change material on the performance of air-conditioning unit. *Appl. Energy* **2018**, *230*, 1380–1402, doi:10.1016/j.apenergy.2018.09.048.
26. Alehosseini, E.; Jafari, S.M. Micro/nano-encapsulated phase change materials (PCMs) as emerging materials for the food industry. *Trends Food Sci. Technol.* **2019**, *91*, 116–128.
27. Lv, Y.; Zou, Y.; Yang, L. Feasibility study for thermal protection by microencapsulated phase change micro/nanoparticles during cryosurgery. *Chem. Eng. Sci.* **2011**, *66*, 3941–3953, doi:10.1016/j.ces.2011.05.031.
28. Magendran, S.S.; Khan, F.S.A.; Mubarak, N.M.; Vaka, M.; Walvekar, R.; Khalid, M.; Abdullah, E.C.; Nizamuddin, S.; Karri, R.R. Synthesis of organic phase change materials (PCM) for energy storage applications: A review. *Nano-Struct. Nano-Objects* **2019**, *20*, doi:10.1016/j.nanoso.2019.100399.
29. Pielichowska, K.; Pielichowski, K. Phase change materials for thermal energy storage. *Prog. Mater. Sci.* **2014**, *65*, 67–123, doi:10.1016/j.pmatsci.2014.03.005.
30. Du, K.; Calautit, J.; Wang, Z.; Wu, Y.; Liu, H. A review of the applications of phase change materials in cooling, heating and power generation in different temperature ranges. *Appl. Energy* **2018**, *220*, 242–273, doi:10.1016/j.apenergy.2018.03.005.
31. Li, S.F.; Liu, Z. hua; Wang, X.J. A comprehensive review on positive cold energy storage technologies and applications in air conditioning with phase change materials. *Appl. Energy* **2019**, *255*, doi:10.1016/j.apenergy.2019.113667.
32. Fernández, A.I.; Barreneche, C.; Belusko, M.; Segarra, M.; Bruno, F.; Cabeza, L.F. Considerations for the use of metal alloys as phase change materials for high temperature applications. *Sol. Energy Mater. Sol. Cells* **2017**, *171*, 275–281, doi:10.1016/j.solmat.2017.06.054.
33. Kadivar, M.R.; Moghimi, M.A.; Sapin, P.; Markides, C.N. Annulus eccentricity optimisation of a phase-change material (PCM) horizontal double-pipe thermal energy store. *J. Energy Storage* **2019**, *26*, doi:10.1016/j.est.2019.101030.

34. Wu, S.; Yan, T.; Kuai, Z.; Pan, W. Thermal conductivity enhancement on phase change materials for thermal energy storage: A review. *Energy Storage Mater.* **2020**, *25*, 251–295, doi:10.1016/j.ensm.2019.10.010.
35. Liu, L.; Su, D.; Tang, Y.; Fang, G. Thermal conductivity enhancement of phase change materials for thermal energy storage: A review. *Renew. Sustain. Energy Rev.* **2016**, *62*, 305–317.
36. Rehman, T. ur; Ali, H.M.; Janjua, M.M.; Sajjad, U.; Yan, W.M. A critical review on heat transfer augmentation of phase change materials embedded with porous materials/foams. *Int. J. Heat Mass Transf.* **2019**, *135*, 649–673, doi:10.1016/j.ijheatmasstransfer.2019.02.001.
37. Qureshi, Z.A.; Ali, H.M.; Khushnood, S. Recent advances on thermal conductivity enhancement of phase change materials for energy storage system: A review. *Int. J. Heat Mass Transf.* **2018**, *127*, 838–856, doi:10.1016/j.ijheatmasstransfer.2018.08.049.
38. Lin, Y.; Jia, Y.; Alva, G.; Fang, G. Review on thermal conductivity enhancement, thermal properties and applications of phase change materials in thermal energy storage. *Renew. Sustain. Energy Rev.* **2018**, *82*, 2730–2742, doi:10.1016/j.rser.2017.10.002.
39. Eanest Jebasingh, B.; Valan Arasu, A. A comprehensive review on latent heat and thermal conductivity of nanoparticle dispersed phase change material for low-temperature applications. *Energy Storage Mater.* **2020**, *24*, 52–74, doi:10.1016/j.ensm.2019.07.031.
40. Leong, K.Y.; Abdul Rahman, M.R.; Gurunathan, B.A. Nano-enhanced phase change materials: A review of thermo-physical properties, applications and challenges. *J. Energy Storage* **2019**, *21*, 18–31, doi:10.1016/j.est.2018.11.008.
41. Wang, Y.; Zhang, X.; Ji, J.; Li, Y.; Munyalo, J.M.; Liu, B.; Xu, X.; Liu, S. Thermal conductivity modification of n-octanoic acid-myristic acid composite phase change material. *J. Mol. Liq.* **2019**, *288*, doi:10.1016/j.molliq.2019.111092.
42. Lin, S.C.; Al-Kayiem, H.H. Evaluation of copper nanoparticles—Paraffin wax compositions for solar thermal energy storage. *Sol. Energy* **2016**, *132*, 267–278, doi:10.1016/j.solener.2016.03.004.
43. Sami, S.; Etesami, N. Improving thermal characteristics and stability of phase change material containing TiO2 nanoparticles after thermal cycles for energy storage. *Appl. Therm. Eng.* **2017**, *124*, 346–352, doi:10.1016/j.applthermaleng.2017.06.023.
44. Soni, V.; Kumar, A.; Jain, V.K. Performance evaluation of nano-enhanced phase change materials during discharge stage in waste heat recovery. *Renew. Energy* **2018**, *127*, 587–601, doi:10.1016/j.renene.2018.05.009.
45. Martín, M.; Villalba, A.; Inés Fernández, A.; Barreneche, C. Development of new nano-enhanced phase change materials (NEPCM) to improve energy efficiency in buildings: Lab-scale characterization. *Energy Build.* **2019**, *192*, 75–83, doi:10.1016/j.enbuild.2019.03.029.
46. Masoumi, H.; Haghighi khoshkhoo, R.; Mirfendereski, S.M. Modification of physical and thermal characteristics of stearic acid as a phase change materials using TiO_2-nanoparticles. *Thermochim. Acta* **2019**, *675*, 9–17, doi:10.1016/j.tca.2019.02.015.
47. Ali, M.A.; Fayaz; Viegas, R.F.; Shyam Kumar, M.B.; Kannapiran, R.K.; Feroskhan, M. Enhancement of heat transfer in paraffin wax PCM using nano graphene composite for industrial helmets. *J. Energy Storage* **2019**, *26*, doi:10.1016/j.est.2019.100982.
48. Salyan, S.; Suresh, S. Study of thermo-physical properties and cycling stability of D-Mannitol-copper oxide nanocomposites as phase change materials. *J. Energy Storage* **2018**, *15*, 245–255, doi:10.1016/j.est.2017.10.013.
49. Mishra, A.K.; Lahiri, B.B.; Philip, J. Thermal conductivity enhancement in organic phase change material (phenol-water system) upon addition of Al_2O_3, SiO_2 and TiO_2 nano-inclusions. *J. Mol. Liq.* **2018**, *269*, 47–63, doi:10.1016/j.molliq.2018.08.001.
50. Águila V.B.; Vasco, D.A.; Galvez P.P.; Zapata, P.A.; V, B.Á.; Vasco, D.A.; P.P.G.; Zapata, P.A. Effect of temperature and CuO-nanoparticle concentration on the thermal conductivity and viscosity of an organic phase-change material. *Int. J. Heat Mass Transf.* **2018**, *120*, 1009–1019, doi:10.1016/j.ijheatmasstransfer.2017.12.106.
51. Mishra, A.K.; Lahiri, B.B.; Solomon, V.; Philip, J. Nano-inclusion aided thermal conductivity enhancement in palmitic acid/di-methyl formamide phase change material for latent heat thermal energy storage. *Thermochim. Acta* **2019**, *678*, doi:10.1016/j.tca.2019.178309.
52. Choi, D.H.; Lee, J.; Hong, H.; Kang, Y.T. Thermal conductivity and heat transfer performance enhancement of phase change materials (PCM) containing carbon additives for heat storage application. *Int. J. Refrig.* **2014**, *42*, 112–120, doi:10.1016/j.ijrefrig.2014.02.004.

53. Vivekananthan, M.; Amirtham, V.A. Characterisation and thermophysical properties of graphene nanoparticles dispersed erythritol PCM for medium temperature thermal energy storage applications. *Thermochim. Acta* **2019**, *676*, 94–103, doi:10.1016/j.tca.2019.03.037.
54. He, M.; Yang, L.; Lin, W.; Chen, J.; Mao, X.; Ma, Z. Preparation, thermal characterization and examination of phase change materials (PCMs) enhanced by carbon-based nanoparticles for solar thermal energy storage. *J. Energy Storage* **2019**, *25*, doi:10.1016/j.est.2019.100874.
55. Liu, Y.; Liu, W.; Zhang, S.; Tian, D.; Tian, Z. Preparation and characterization of new nano-particle mixed as thermal storage material. *Appl. Therm. Eng.* **2019**, *163*, doi:10.1016/j.applthermaleng.2019.114386.
56. Al Ghossein, R.M.; Hossain, M.S.; Khodadadi, J.M. Experimental determination of temperature-dependent thermal conductivity of solid eicosane-based silver nanostructure-enhanced phase change materials for thermal energy storage. *Int. J. Heat Mass Transf.* **2017**, *107*, 697–711, doi:10.1016/j.ijheatmasstransfer.2016.11.059.
57. Gupta, N.; Kumar, A.; Dhawan, S.K.; Dhasmana, H.; Kumar, A.; Kumar, V.; Verma, A.; Jain, V.K. Metal nanoparticles enhanced thermophysical properties of phase change material for thermal energy storage. *Mater. Today Proc.* **2020**, doi:10.1016/j.matpr.2020.02.164.
58. Aslfattahi, N.; Saidur, R.; Arifutzzaman, A.; Sadri, R.; Bimbo, N.; Sabri, M.F.M.; Maughan, P.A.; Bouscarrat, L.; Dawson, R.J.; Said, S.M.; et al. Experimental investigation of energy storage properties and thermal conductivity of a novel organic phase change material/MXene as A new class of nanocomposites. *J. Energy Storage* **2020**, *27*, doi:10.1016/j.est.2019.101115.
59. Zhu, X.; Han, L.; Lu, Y.; Wei, F.; Jia, X. Geometry-induced thermal storage enhancement of shape-stabilized phase change materials based on oriented carbon nanotubes. *Appl. Energy* **2019**, *254*, doi:10.1016/j.apenergy.2019.113688.
60. Prabakaran, R.; Sidney, S.; Lal, D.M.; Selvam, C.; Harish, S. Solidification of Graphene-Assisted Phase Change Nanocomposites inside a Sphere for Cold Storage Applications. *Energies* **2019**, *12*, 3473, doi:10.3390/en12183473.
61. Ranjbar, S.G.; Roudini, G.; Barahuie, F. Fabrication and characterization of phase change material-SiO2 nanocomposite for thermal energy storage in buildings. *J. Energy Storage* **2020**, *27*, doi:10.1016/j.est.2019.101168.
62. Frusteri, F.; Leonardi, V.; Vasta, S.; Restuccia, G. Thermal conductivity measurement of a PCM based storage system containing carbon fibers. *Appl. Therm. Eng.* **2005**, *25*, 1623–1633, doi:10.1016/j.applthermaleng.2004.10.007.
63. Xiao, X.; Zhang, P.; Li, M. Effective thermal conductivity of open-cell metal foams impregnated with pure paraffin for latent heat storage. *Int. J. Therm. Sci.* **2014**, *81*, 94–105, doi:10.1016/j.ijthermalsci.2014.03.006.
64. Wang, Z.; Zhang, Z.; Jia, L.; Yang, L. Paraffin and paraffin/aluminum foam composite phase change material heat storage experimental study based on thermal management of Li-ion battery. *Appl. Therm. Eng.* **2015**, *78*, 428–436, doi:10.1016/j.applthermaleng.2015.01.009.
65. Fleming, E.; Wen, S.; Shi, L.; Da Silva, A.K. Experimental and theoretical analysis of an aluminum foam enhanced phase change thermal storage unit. *Int. J. Heat Mass Transf.* **2015**, *82*, 273–281, doi:10.1016/j.ijheatmasstransfer.2014.11.022.
66. Huang, X.; Lin, Y.; Alva, G.; Fang, G. Thermal properties and thermal conductivity enhancement of composite phase change materials using myristyl alcohol/metal foam for solar thermal storage. *Sol. Energy Mater. Sol. Cells* **2017**, *170*, 68–76, doi:10.1016/j.solmat.2017.05.059.
67. Li, T.X.; Wu, D.L.; He, F.; Wang, R.Z. Experimental investigation on copper foam/hydrated salt composite phase change material for thermal energy storage. *Int. J. Heat Mass Transf.* **2017**, *115*, 148–157, doi:10.1016/j.ijheatmasstransfer.2017.07.056.
68. Xiao, X.; Zhang, P.; Li, M. Preparation and thermal characterization of paraffin/metal foam composite phase change material. *Appl. Energy* **2013**, *112*, 1357–1366, doi:10.1016/j.apenergy.2013.04.050.
69. Righetti, G.; Lazzarin, R.; Noro, M.; Mancin, S. Phase change materials embedded in porous matrices for hybrid thermal energy storages: Experimental results and modeling Résultats expérimentaux et modélisation concernant des matériaux à changement de phase incorporées dans des matrices poreuses pour. *Int. J. Refrig.* **2019**, *106*, 266–277.
70. Zheng, H.; Wang, C. Numerical and Experimental Studies on the Heat Transfer Performance of Copper Foam Filled with Paraffin. *Energies* **2017**, *10*, 902, doi:10.3390/en10070902.

71. Zhu, C.; Ran, F.; Fang, G. Thermal properties improvement of lauric acid/iron foam composites with graphene nanoplates as thermal energy storage materials. *J. Energy Storage* **2020**, *27*, doi:10.1016/j.est.2019.101163.
72. Yang, X.; Wei, P.; Cui, X.; Jin, L.; He, Y.L. Thermal response of annuli filled with metal foam for thermal energy storage: An experimental study. *Appl. Energy* **2019**, *250*, 1457–1467, doi:10.1016/j.apenergy.2019.05.096.
73. Liu, Y.; Duan, J.; He, X.; Wang, Y. Experimental investigation on the heat transfer enhancement in a novel latent heat thermal storage equipment. *Appl. Therm. Eng.* **2018**, *142*, 361–370, doi:10.1016/j.applthermaleng.2018.07.009.
74. Chen, X.; Li, X.; Xia, X.; Sun, C.; Liu, R. Thermal Performance of a PCM-Based Thermal Energy Storage with Metal Foam Enhancement. *Energies* **2019**, *12*, 3275, doi:10.3390/en12173275.
75. Xu, Y.; Li, M.J.; Zheng, Z.J.; Xue, X.D. Melting performance enhancement of phase change material by a limited amount of metal foam: Configurational optimization and economic assessment. *Appl. Energy* **2018**, *212*, 868–880, doi:10.1016/j.apenergy.2017.12.082.
76. Gasia, J.; Maldonado, J.M.; Galati, F.; De Simone, M.; Cabeza, L.F. Experimental evaluation of the use of fins and metal wool as heat transfer enhancement techniques in a latent heat thermal energy storage system. *Energy Convers. Manag.* **2019**, *184*, 530–538, doi:10.1016/j.enconman.2019.01.085.
77. Fukai, J.; Kanou, M.; Kodama, Y.; Miyatake, O. Thermal conductivity enhancement of energy storage media using carbon fibers. *Energy Convers. Manag.* **2000**, *41*, 1543–1556, doi:10.1016/S0196-8904(99)00166-1.
78. Cheng, F.; Zhang, X.; Wen, R.; Huang, Z.; Fang, M.; Liu, Y.; Wu, X.; Min, X. Thermal conductivity enhancement of form-stable tetradecanol/expanded perlite composite phase change materials by adding Cu powder and carbon fiber for thermal energy storage. *Appl. Therm. Eng.* **2019**, *156*, 653–659, doi:10.1016/j.applthermaleng.2019.03.140.
79. Zhang, Q.; Luo, Z.; Guo, Q.; Wu, G. Preparation and thermal properties of short carbon fibers/erythritol phase change materials. *Energy Convers. Manag.* **2017**, *136*, 220–228, doi:10.1016/j.enconman.2017.01.023.
80. Lu, W.; Liu, G.; Xiong, Z.; Wu, Z.; Zhang, G. An experimental investigation of composite phase change materials of ternary nitrate and expanded graphite for medium-temperature thermal energy storage. *Sol. Energy* **2020**, *195*, 573–580, doi:10.1016/j.solener.2019.11.102.
81. Fu, W.; Zou, T.; Liang, X.; Wang, S.; Gao, X.; Zhang, Z.; Fang, Y. Thermal properties and thermal conductivity enhancement of composite phase change material using sodium acetate trihydrate–urea/expanded graphite for radiant floor heating system. *Appl. Therm. Eng.* **2018**, *138*, 618–626, doi:10.1016/j.applthermaleng.2018.04.102.
82. Yuan, M.; Ren, Y.; Xu, C.; Ye, F.; Du, X. Characterization and stability study of a form-stable erythritol/expanded graphite composite phase change material for thermal energy storage. *Renew. Energy* **2019**, *136*, 211–222, doi:10.1016/j.renene.2018.12.107.
83. Wu, W.; Wu, W.; Wang, S. Form-stable and thermally induced flexible composite phase change material for thermal energy storage and thermal management applications. *Appl. Energy* **2019**, *236*, 10–21, doi:10.1016/j.apenergy.2018.11.071.
84. Kenisarin, M.; Mahkamov, K.; Kahwash, F.; Makhkamova, I. Enhancing thermal conductivity of paraffin wax 53–57 °C using expanded graphite. *Sol. Energy Mater. Sol. Cells* **2019**, *200*, doi:10.1016/j.solmat.2019.110026.
85. Zhang, X.; Zhu, C.; Fang, G. Preparation and thermal properties of n-eicosane/nano-SiO_2/expanded graphite composite phase-change material for thermal energy storage. *Mater. Chem. Phys.* **2020**, *240*, doi:10.1016/j.matchemphys.2019.122178.
86. Xiao, Q.; Yuan, W.; Li, L.; Xu, T. Fabrication and characteristics of composite phase change material based on $Ba(OH)_2{\cdot}8H_2O$ for thermal energy storage. *Sol. Energy Mater. Sol. Cells* **2018**, *179*, 339–345, doi:10.1016/j.solmat.2017.12.032.
87. Ren, Y.; Li, P.; Yuan, M.; Ye, F.; Xu, C.; Liu, Z. Effect of the fabrication process on the thermophysical properties of $Ca(NO_3)_2$–$NaNO_3$/expanded graphite phase change material composites. *Sol. Energy Mater. Sol. Cells* **2019**, *200*, doi:10.1016/j.solmat.2019.110005.
88. Qu, Y.; Wang, S.; Tian, Y.; Zhou, D. Comprehensive evaluation of Paraffin-HDPE shape stabilized PCM with hybrid carbon nano-additives. *Appl. Therm. Eng.* **2019**, *163*, doi:10.1016/j.applthermaleng.2019.114404.
89. Li, C.; Yu, H.; Song, Y.; Wang, M.; Liu, Z. A n-octadecane/hierarchically porous TiO2 form-stable PCM for thermal energy storage. *Renew. Energy* **2020**, *145*, 1465–1473, doi:10.1016/j.renene.2019.06.070.

90. Li, R.; Zhou, Y.; Duan, X. A novel composite phase change material with paraffin wax in tailings porous ceramics. *Appl. Therm. Eng.* **2019**, *151*, 115–123, doi:10.1016/j.applthermaleng.2019.01.104.
91. Li, C.; Li, Q.; Cong, L.; jiang, F.; Zhao, Y.; Liu, C.; Xiong, Y.; Chang, C.; Ding, Y. MgO based composite phase change materials for thermal energy storage: The effects of MgO particle density and size on microstructural characteristics as well as thermophysical and mechanical properties. *Appl. Energy* **2019**, *250*, 81–91, doi:10.1016/j.apenergy.2019.04.094.
92. Gu, X.; Liu, P.; Bian, L.; He, H. Enhanced thermal conductivity of palmitic acid/mullite phase change composite with graphite powder for thermal energy storage. *Renew. Energy* **2019**, *138*, 833–841, doi:10.1016/j.renene.2019.02.031.
93. Chen, B.; Han, M.; Zhang, B.; Ouyang, G.; Shafei, B.; Wang, X.; Hu, S. Efficient Solar-to-Thermal Energy Conversion and Storage with High-Thermal-Conductivity and Form-Stabilized Phase Change Composite Based on Wood-Derived Scaffolds. *Energies* **2019**, *12*, 1283, doi:10.3390/en12071283.
94. Qu, Y.; Wang, S.; Zhou, D.; Tian, Y. Experimental study on thermal conductivity of paraffin-based shape-stabilized phase change material with hybrid carbon nano-additives. *Renew. Energy* **2020**, *146*, 2637–2645, doi:10.1016/j.renene.2019.08.098.
95. Shuja, S.Z.; Yilbas, B.S.; Shaukat, M.M. Melting enhancement of a phase change material with presence of a metallic mesh. *Appl. Therm. Eng.* **2015**, *79*, 163–173, doi:10.1016/j.applthermaleng.2015.01.033.
96. Duan, J.; Xiong, Y.; Yang, D. Melting Behavior of Phase Change Material in Honeycomb Structures with Different Geometrical Cores. *Energies* **2019**, *12*, 2920, doi:10.3390/en12152920.
97. Singh, R.; Sadeghi, S.; Shabani, B. Thermal Conductivity Enhancement of Phase Change Materials for Low-Temperature Thermal Energy Storage Applications. *Energies* **2019**, *12*, 75, doi:10.3390/en12010075.
98. Liu, Z.; Yu, Z. (Jerry); Yang, T.; Qin, D.; Li, S.; Zhang, G.; Haghighat, F.; Joybari, M.M. A review on macro-encapsulated phase change material for building envelope applications. *Build. Environ.* **2018**, *144*, 281–294, doi:10.1016/j.buildenv.2018.08.030.
99. Delgado, M.; Lázaro, A.; Mazo, J.; Zalba, B. Review on phase change material emulsions and microencapsulated phase change material slurries: Materials, heat transfer studies and applications. *Renew. Sustain. Energy Rev.* **2012**, *16*, 253–273, doi:10.1016/j.rser.2011.07.152.
100. Zhu, Y.; Qin, Y.; Liang, S.; Chen, K.; Tian, C.; Wang, J.; Luo, X.; Zhang, L. Graphene/SiO_2/n-octadecane nanoencapsulated phase change material with flower like morphology, high thermal conductivity, and suppressed supercooling. *Appl. Energy* **2019**, *250*, 98–108, doi:10.1016/j.apenergy.2019.05.021.
101. Zhong, Y.; Zhao, B.; Lin, J.; Zhang, F.; Wang, H.; Zhu, Z.; Dai, Z. Encapsulation of high-temperature inorganic phase change materials using graphite as heat transfer enhancer. *Renew. Energy* **2019**, *133*, 240–247, doi:10.1016/j.renene.2018.09.107.
102. Zhang, Z.; Lian, Y.; Xu, X.; Xu, X.; Fang, G.; Gu, M. Synthesis and characterization of microencapsulated sodium sulfate decahydrate as phase change energy storage materials. *Appl. Energy* **2019**, *255*, doi:10.1016/j.apenergy.2019.113830.
103. Yu, S.; Wang, X.; Wu, D. Microencapsulation of n-octadecane phase change material with calcium carbonate shell for enhancement of thermal conductivity and serving durability: Synthesis, microstructure, and performance evaluation. *Appl. Energy* **2014**, *114*, 632–643, doi:10.1016/j.apenergy.2013.10.029.
104. Cheng, T.; Wang, N.; Wang, H.; Sun, R.; Wong, C.P. A newly designed paraffin@VO2 phase change material with the combination of high latent heat and large thermal conductivity. *J. Colloid Interface Sci.* **2020**, *559*, 226–235, doi:10.1016/j.jcis.2019.10.033.
105. Zhu, Y.; Qin, Y.; Wei, C.; Liang, S.; Luo, X.; Wang, J.; Zhang, L. Nanoencapsulated phase change materials with polymer-SiO_2 hybrid shell materials: Compositions, morphologies, and properties. *Energy Convers. Manag.* **2018**, *164*, 83–92, doi:10.1016/j.enconman.2018.02.075.
106. Xia, Y.; Cui, W.; Ji, R.; Huang, C.; Huang, Y.; Zhang, H.; Xu, F.; Huang, P.; Li, B.; Sun, L. Design and synthesis of novel microencapsulated phase change materials with enhancement of thermal conductivity and thermal stability: Self-assembled boron nitride into shell materials. *Colloids Surfaces A Physicochem. Eng. Asp.* **2020**, *586*, 124225, doi:10.1016/j.colsurfa.2019.124225.
107. Wang, X.; Li, C.; Zhao, T. Fabrication and characterization of poly(melamine-formaldehyde)/silicon carbide hybrid microencapsulated phase change materials with enhanced thermal conductivity and light-heat performance. *Sol. Energy Mater. Sol. Cells* **2018**, *183*, 82–91, doi:10.1016/j.solmat.2018.03.019.

108. Praveen, B.; Suresh, S.; Pethurajan, V. Heat transfer performance of graphene nano-platelets laden micro-encapsulated PCM with polymer shell for thermal energy storage based heat sink. *Appl. Therm. Eng.* **2019**, *156*, 237–249, doi:10.1016/j.applthermaleng.2019.04.072.
109. Jia, X.; Zhai, X.; Cheng, X. Thermal performance analysis and optimization of a spherical PCM capsule with pin-fins for cold storage. *Appl. Therm. Eng.* **2019**, *148*, 929–938, doi:10.1016/j.applthermaleng.2018.11.105.
110. Puertas, A.M.; Romero-Cano, M.S.; De Las Nieves, F.J.; Rosiek, S.; Batlles, F.J. Simulations of Melting of Encapsulated $CaCl_2 \bullet 6H_2O$ for Thermal Energy Storage Technologies. *Energies* **2017**, *10*, 568, doi:10.3390/en10040568.
111. Feng, G.H.; Liang, D.; Huang, K.L.; Wang, Y. Thermal performance difference of phase change energy storage units based on tubular macro-encapsulation. *Sustain. Cities Soc.* **2019**, *50*, doi:10.1016/j.scs.2019.101662.
112. Zhang, H.; Wang, X.; Wu, D. Silica encapsulation of n-octadecane via sol-gel process: A novel microencapsulated phase-change material with enhanced thermal conductivity and performance. *J. Colloid Interface Sci.* **2010**, *343*, 246–255, doi:10.1016/j.jcis.2009.11.036.